WOOD PLASTIC COMPOSITE SILL PLATE FOR CONTINUOUS ANCHORAGE OF SHEAR WALLS IN LIGHT-FRAME WOOD STRUCTURES

By

JASON O'DELL

A thesis submitted in partial fulfillment of
the requirements for the degree of

MASTER OF SCIENCE IN CIVIL ENGINEERING

WASHINGTON STATE UNIVERSITY
Department of Civil and Environmental Engineering

AUGUST 2008

To the Faculty of Washington State University:

The Members of the Committee appointed to examine the thesis of JASON O'DELL find it satisfactory and recommend that it be accepted.

_____
Chair

_____

_____

ACKNOWLEDGEMENT

First, I would like to thank the Office of Naval Research for funding this project (under contract N00014-06-1-0874) and allowing me to take on this endeavor. It has been a valuable learning experience.

Next, I would like to thank my colleagues at Washington State University for their support and guidance throughout this project. In particular, I would like to thank Dr. J. Daniel Dolan for his guidance on the direction of this project and sharing his vast knowledge of shear wall behavior; Dr. William Cofer for his guidance on the finite element method and computer modeling; Dr. Karl Englund for his guidance on the properties and behavior of wood plastic composites; and Scott Lewis for his technical advice and assistance in conducting the testing needed to accomplish the goals of this research.

Finally, I would like to thank my family; my wife, Teresa, for her support and understanding through the long hours of schoolwork and my parents for instilling in me the determination and work ethics that have allowed me to accomplish anything that I have ever set my mind to.

WOOD PLASTIC COMPOSITE SILL PLATE FOR CONTINUOUS ANCHORAGE OF SHEAR WALLS IN LIGHT-FRAME WOOD STRUCTURES

Abstract

By Jason O'Dell, M.S.
Washington State University
August 2008

Chair: J. Daniel Dolan

Past research and post-disaster investigations have exposed a few shortcomings in the use of wood sill plates in light-frame wood shear walls. The first is the fact that uplift forces, caused by overturning resistance, induce cross-grain bending in sill plates due to forces from the sheathing-to-sill plate connectors lifting the edge of the sill plate. This bending along the line of anchor bolts often times results in splitting of the sill plate and loss of lateral resistance. The second is wood's inherent property to decay when exposed to moisture and a sill plate's highly exposed nature to moisture. Past studies have also shown that wood plastic composites (WPCs) can be utilized to reduce these problems and are a viable substitution for typical wood sill plates.

In this thesis, a concept of continuous anchorage of a WPC sill plate to improve the performance of light-frame wood shear walls is pursued. This was accomplished by the modeling of a WPC sill plate which included a fin along the bottom edge that can be embedded in a concrete foundation instead of the use of anchor bolts. This embedment into the foundation of a structure will provide continuous anchorage of the shear wall.

This thesis contains the development of a finite element model that is useful for investigating the behavior of a WPC sill plate that has been designed for continuous anchorage of light-frame wood shear walls. The model was verified using a slightly modified cross-section that was easily manufactured and tested.

The resulting model indicates that the continuous anchorage concept is viable. Shear walls with continuous anchorage showed a doubling in strength over unrestrained shear walls built by current prescriptive methods, and are comparable in strength to shear walls with traditional overturning restraint.

TABLE OF CONTENTS

TABLE OF FIGURES

TABLE OF TABLES

CHAPTER 1: INTRODUCTION

1.1 Problem Overview

Historically, light-frame wood structures were thought to perform quite well during seismic activity due to their low mass and high redundancy. The 1994 Northridge Earthquake corrected this perception by leaving 25,000 dwellings uninhabitable, 7,000 buildings red-tagged, 22,000 buildings yellow-tagged, and 9 hospitals closed, making it the most costly natural disaster up to the time of its occurrence (DIS 2007).

The investigations following the disaster showed that in many instances a significant amount of moisture had made its way up between the foundation and the external cladding, significantly reducing the strength of shear walls in light-frame wood structures. With a main component of the lateral force resisting system damaged by decay, an entire structure becomes dangerous. Adding to the hazard of this situation is the fact that shear wall damage is concealed within the walls, and is often not discovered until it is too late (i.e., post-disaster investigations).

Structural damage resulting from moisture infiltration is also quite costly monetarily. A few of the more significant cases in the last decade are, "leaky condominiums of Vancouver [British Columbia] that involved over CDN $1 Billion in damages, decay in sheathing in North Carolina that involved the class action settlement of US $20 million in 1998, decay in framing and sheathing in leaky condominiums in Seattle with damage over US $100 million" (CRD 2007). The extent of this problem was well stated by Kubal (2000) when he said that moisture problems "damage or completely destroy more buildings and structures than war or natural disaster".

In the United States, 80-90% of all structures are of wood-frame construction. In Los Angeles County alone (where the Northridge Earthquake struck), 81% of structures and 99% of residences are of wood-frame construction (Mahaney and Kehoe 2002). With such a large percentage of the population living and working in wood-frame structures, it is apparent that something needs to be done to reduce this moisture damage problem.

The results of the Northridge Earthquake sparked massive changes in the engineering world. One of these changes has been to take a closer look at the behavior of shear walls and their components under cyclic loading. In 2002, the Consortium of Universities for Research in Earthquake Engineering (CUREE), conducted tests on wood-frame shear wall assemblies. Out of the sixty-three valid tests, thirty-four of them failed at the sill plate (Mahaney and Kehoe 2002). Sill plate failures are often a result of the eccentricity of the sheathing-to-sill plate connectors pulling up on one side of the sill plate cross-section while anchor bolts hold the sill plate down to the foundation of floor platform along the centerline. This results in a tension failure on the bottom side of the sill plate and runs parallel to the grain as can be seen in Figure 1.1. These tests did not take into account the loss of strength that occurs when wood members have been affected by decay.

One thing that several building codes have done to decrease moisture damage to this critical, yet highly exposed, element is to require treated lumber for structural elements in contact with concrete foundations. But because of environmental and fastener corrosion issues, treated lumber is becoming increasingly costly and more difficult to work with.

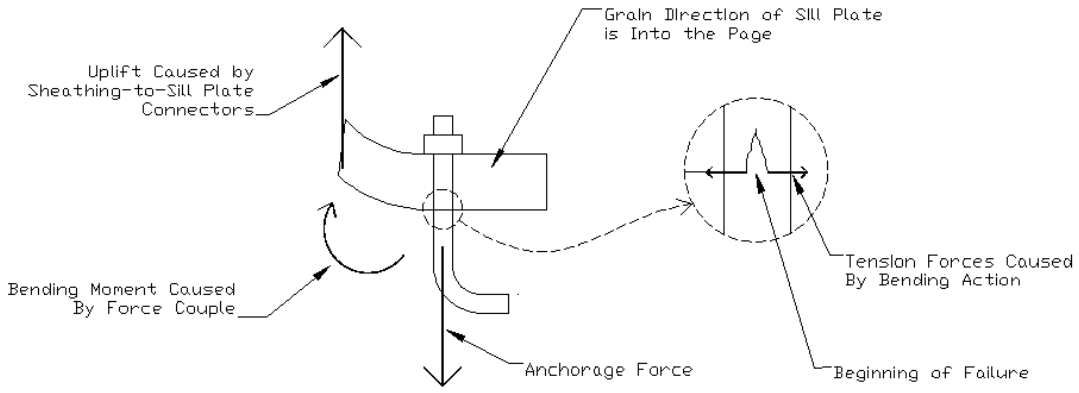

Figure 1. 1: Cross-Grain Bending of a Traditional Wood Sill Plate

1.2 Background

1.2.1 Shear Walls

Shear wall are primarily used to resist lateral forces, such as those induced on a structure by wind and earthquakes. In addition to this, shear walls also transfer gravity loads. A light-frame wood shear wall is typically composed of three components; 1) framing, 2) sheathing, and 3) framing-to-sheathing connectors. Also important to bottom story shear wall performance, but technically not a component of the shear wall itself, is the foundation-to-framing connection. This study focused on a combined framing/foundation-to-framing connection member by investigating a sill plate that will be embedded in the concrete foundation. This is discussed further in Section 1.2.3.

The load path of a common lateral force resisting system is depicted in Figure 1.2. Horizontal loads are transferred to the floor diaphragm through out-of-plane bending of

the walls transverse to the load. From the diaphragm, the load is transferred to the walls parallel to the load. These are the shear walls. The shear walls then transfers the load to the foundation and earth through the foundation-to-framing connectors.

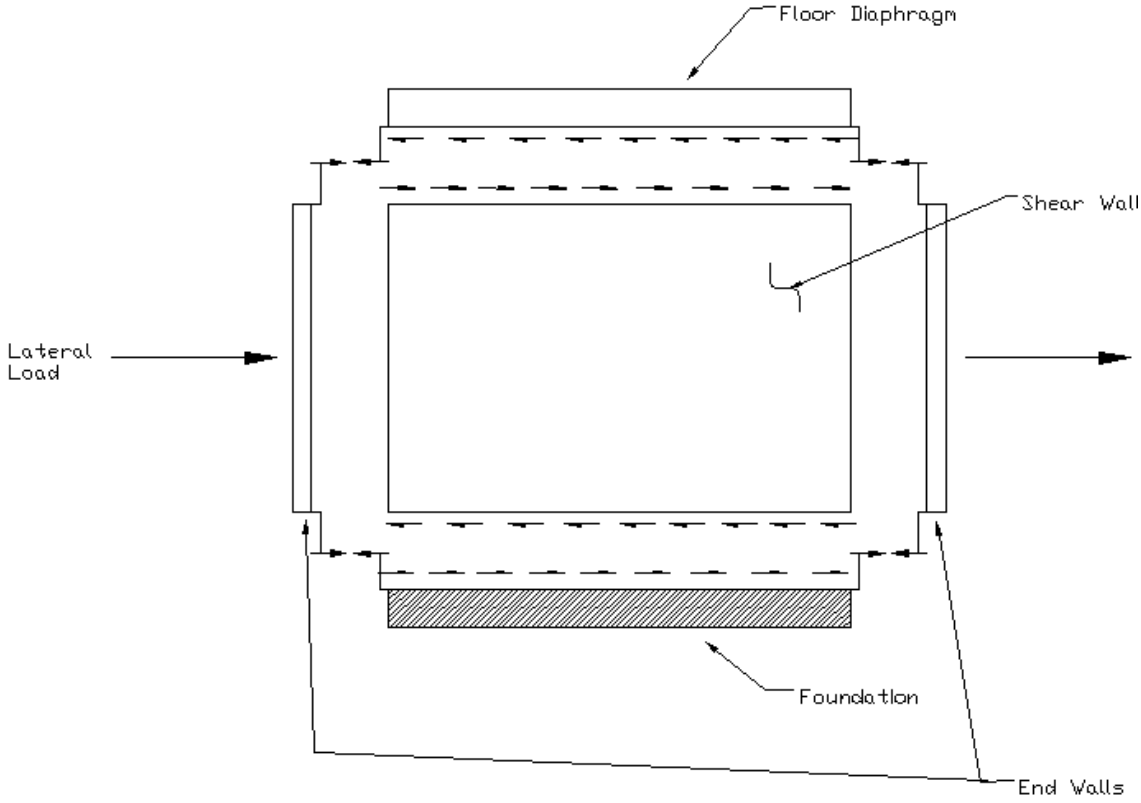

Figure 1. 2: Load Path of Lateral Loads Through a Common Light-Frame Lateral Force Resisting System

Typical framing for a light-frame wood shear wall is composed of either 2X4 or 2X6 nominal lumber. The species of wood used depends on what is available in the location of construction. Studies have shown that the framing does not add significantly to the in-plane stiffness of a shear wall (Dolan 1989). Sheathing is typically a panel-type wood product such as plywood or oriented strand board (OSB). It is the sheathing that transfers the lateral forces of a typical shear wall system (Bredel 2003). The typical framing-to-sheathing connector elements are dowel-type fasteners such as nails or

staples. It has been long understood that the framing-to-sheathing connector elements are the most important factor in determining the strength and stiffness of shear walls (Foschi 1977; McCutcheon 1985; Dowrick 1986; Stewart 1987; Dolan 1989; Dolan and Madsen 1992; Heine 1997). A typical assembled shear wall is shown in Figure 1.3.

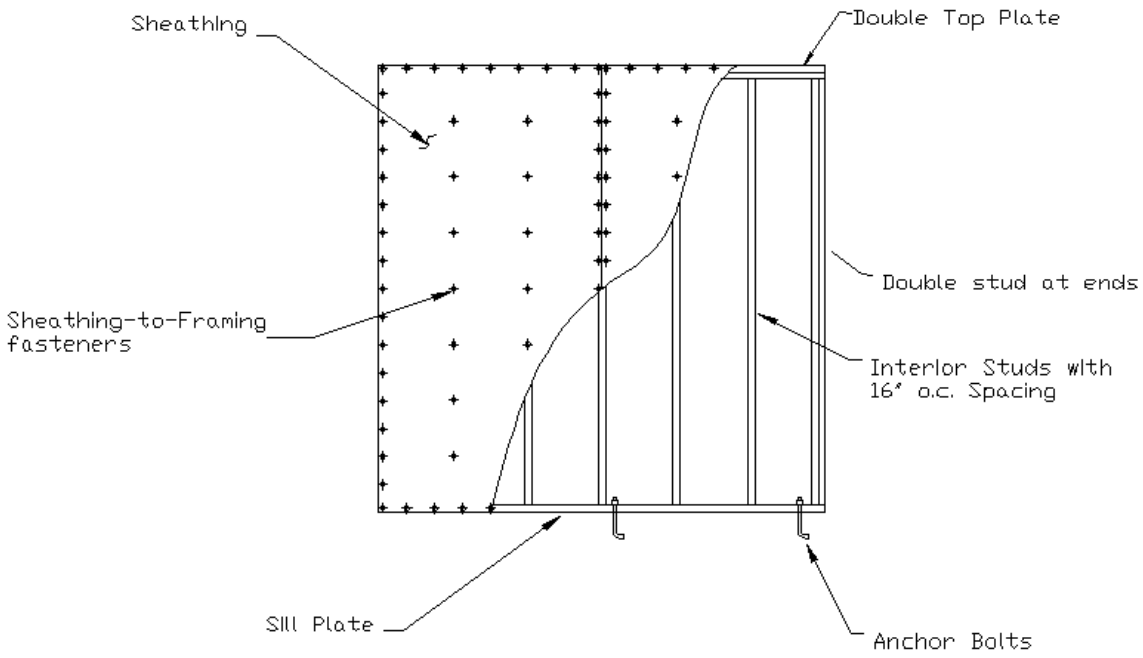

Figure 1. 3: Typical light-frame wood Shear Wall

It was in the 1940's when panel-type sheathing began its rise to popularity. In 1949, design guidelines were published for panel-type sheathing, bringing the modern shear wall into common construction practices. Because the mechanics of panel-type sheathing and shear walls was not well understood, design guidelines were primarily based on experience and testing. Because of the high cost associated with dynamic testing, shear wall research has focused on monotonic performance.

Dolan (1989) did some of the earliest cyclic and shake table testing of shear walls and found that the cyclic response envelope correlated well with the monotonic performance curve. Since then, other researchers have come to the same conclusion.

Because of this, traditionally, shear walls have been designed for earthquake performance (cyclic loading) based on monotonic tests (Salenikovich 1997; Rose 1998).

The investigations following the Northridge Earthquake in 1994 found that shear walls designed based on monotonic performance did not perform as well under cyclic loading as previously thought. In 1995, the City of Los Angles Department of Building and Safety issued an emergency code change that reduced the shear design strength of code-recognized allowable design values for shear walls that were based on monotonic testing by 25% (Rose 1998).

The last decade has seen numerous investigations into various aspects of shear wall performance under cyclic loading.

1.2.2 Shear Wall Finite Element Models

In the last half century, the method of finite elements (FE) has proven to be a superb solution technique to many investigations. Starting in the aeronautics industry in the 1940's, the method rapidly spread to other disciplines. The method has been used for analyzing shear walls since the 1960's (Salenikovich 2000). Because of its versatility and accuracy, the finite element method's popularity soared, and in the 1970's researchers started to use the method to predict stresses, deflections, and ultimate load capacities of walls (Polensek 1976). Around this same time, researchers began to look at the nonlinear behavior of shear wall connections (Foschi 1977). It wasn't until computer technology made some major advances in the 1980's that the finite element method became practical to look at dynamic, pseudo-dynamic, and cyclic shear wall behavior. As the price of computers decreased, finite element analysis became more cost effective

in comparison with physical testing for many research concepts (or at least a cost effective way to start some research).

One of the first shear wall finite element models was put together by Foschi (1977). This model was modified by various researchers. Some of those that proposed new models were Itani and Cheung (1984), Gutkowski and Castillo (1988) and Falk and Itani (1989). However, none of these models accounted for dynamic or cyclic response of shear walls. In 1989, Dolan proposed a model that was capable of looking at the dynamic and cyclic response of shear walls. He also made the model general so that various aspects could be easily investigated. After verification testing, Dolan determined that his model could be simplified to reduce the number of degrees of freedom (DOFs) and reduce computer effort. Then in 1995, White and Dolan simplified Dolan's model. In addition to the reduced number of DOFs that Dolan suggested, this model was also capable of computing a time history of forces and stresses in the framing and sheathing elements.

Commercially available, general use finite element programs have also been evolving over the years. These packages are used by placing points in space, connecting them with the desired type of elements (beam, shell, etc.) which will behave in a certain way, assigning properties to the elements (strength, stiffness, etc.), and applying loading and boundary conditions. These programs are capable of a huge array of applications. This is why these packages were chosen to accomplish the research contained in this thesis.

Over the years, the sheathing-to-framing connectors have been shown to be the controlling factor in most shear wall failures. This has initiated many investigations into

connection behavior (Toothman 2003). Some investigations have shown that the nonlinear, hysteretic response of connections can be described with ten parameters (Foliente 1995; Anderson 2006).

The cost associated with connection tests is drastically lower than the cost of conducting full scale shear wall tests. If the parameters that describe the hysteretic behavior of connectors can be obtained from connection tests, then a finite element model of the shear wall can be created using these parameters and reducing research costs.

In 2006, Xu published results of creating a user defined element type for a finite element program, ABAQUS, which reflects the hysteretic response of framing-to-sheathing connectors. He was able to model the hysteretic behavior of dowel-type connectors with 13 parameters that can be obtained from cyclic connection tests. The research contained in this thesis will make use of this element type in an attempt to create the most accurate finite element model possible.

1.2.3 Wood Plastic Composite Sill Plates

Since the U.S. Navy has such a large inventory of waterfront structures, The Office of Naval Research has been funding research in durable building materials for quite some time.

In 2001, Adcock et al showed that, in Wood Plastic Composite (WPC) formulations, polymers have a negative influence on stiffness and a positive influence on strength, while wood has a positive influence on stiffness and a negative influence on strength. This means that the two materials complement each other well, and with proper engineering an ideal material can be formulated for a wide variety of applications.

Because of this, WPCs are a good candidate for structural applications, venturing out of their traditional use. One year later in 2002, research conducted by Pendleton et al, showed that when formulated properly, WPCs are resistant to fungal related decay. This quality shows that WPCs are an exceptional candidate for use in the construction industry as a means to significantly reduce moisture related failures in wood-frame structures.

In 2005, The Office of Naval Research funded another study at Washington State University, this time conducted by Kristen Duchateau (2005), to investigate the potential of WPCs for use as structural sill plates of shear walls. The results of Duchateau's research showed that straight substitution with WPCs result in racking performance comparable to current prescriptive construction methods in regards to strength. However, the WPC sill plate reduced the ductility of the shear wall. Deformation gives both some warning of imminent failure and less energy release upon fracture (because more energy is dissipated in deforming the material there will be less available to be release when members breaks). This is why engineers always design for ductile behavior. Because of this goal, improvements are needed in the material and/or the cross-section of the member before it can be utilized as a structural member in the construction industry.

In typical slab on grade construction practices, anchor bolts hold the sill plate to the foundation with the studs in between the anchor bolts lifting the sill plate away from the foundation. This type of construction can induce severe bending stresses in sill plates. To reduce this problem, Duchateau recommended that the sill plate be extruded with a fin on the bottom. The fin could be set into the concrete foundation at time of casting. By doing this, continuous anchorage of the sill plate is provided; in turn effectively eliminating the effects of bending stresses. To further increase the strength of

the shear wall system, Duchateau also recommended that the sheathing be connected directly to the sill plate by nailing. This would allow the members of the structural wall to work more as a system than individual components.

The research presented in this paper is a continuation of Duchateau's (2005) research, based on her above two recommendations.

1.3 Motivation

Due to the wide use of light-frame wood structures and the utilization of shear walls as their primary lateral force resisting system, along with wood's inherent property to decay and lose strength when exposed to moisture, the design of shear wall members exposed to moisture (i.e. sill plates) warrants an investigation.

By utilizing WPCs as sill plates for light-frame wood shear walls, the benefits are two-fold. First, WPCs can be extruded in almost any shape desired and can be tailored to the task at hand. Second, when formulated properly, WPCs are not susceptible to moisture related decay.

1.4 Objectives

The purpose of this study was to develop a finite element model to investigate the behavior of a WPC sill plate that provides continuous anchorage and the associated influence on the overall strength and stiffness of light-frame wood shear walls. This study was conducted with the main goal being to increase the performance of light-frame

wood shear walls. This was accomplished by satisfying the following objectives:

- Develop an accurate finite element model that will predict the loads transferred to the conceptual sill plate under cyclic loading.
- Develop a detailed finite element model of the conceptual sill plate to look at stress values and stress distribution over the member.
- Verify the accuracy of the model with physical testing.
- Compare the results of the finite element model to design values and to cyclic testing result of light-frame wood shear walls that are built using common construction practices.

CHAPTER 2: MODEL DEVELOPMENT

For this research, two finite element models were developed. The first was the sill plate model. This was a detailed model of the sill plate alone and was used to investigate the behavior of the sill plate. This model can be used in the future to fine tune the sill plate cross section. The second model was the wall framing model. This was a model of the entire shear wall excluding the sill plate. This model was used to predict the forces expected to be transferred to the sill plate through the nailed connections.

Two models were used in the investigation because a single model would have taken an unreasonably long time to converge to a solution. This is primarily due to the fact that this investigation was concerned with the performance of a conceptual sill plate that has complicated geometry. In order to get a good idea of how the sill plate performs, a fine mesh was required of the model. This fine mesh created a need for considerable computer power. By modeling the sill plate separately, only the steps that produced the highest load transfer between the wall framing and the sill plate (via the framing-to-sill plate connectors and the sheathing-to-sill plate connectors) need to be applied to the sill plate. This reduced the computational run time by orders of magnitude.

2.1 Sill Plate Model

The original concept of the sill plate cross-section is shown in Figure 2.1. This cross-sectional shape was arrived at after a stress concentration analysis. The shape has been idealized using three criteria; 1) efficient use of material, 2) a shape that can be

effectively extruded, and 3) a shape that can accommodate typical construction practices, such as attaching interior cladding and using readily available pre-cut studs.

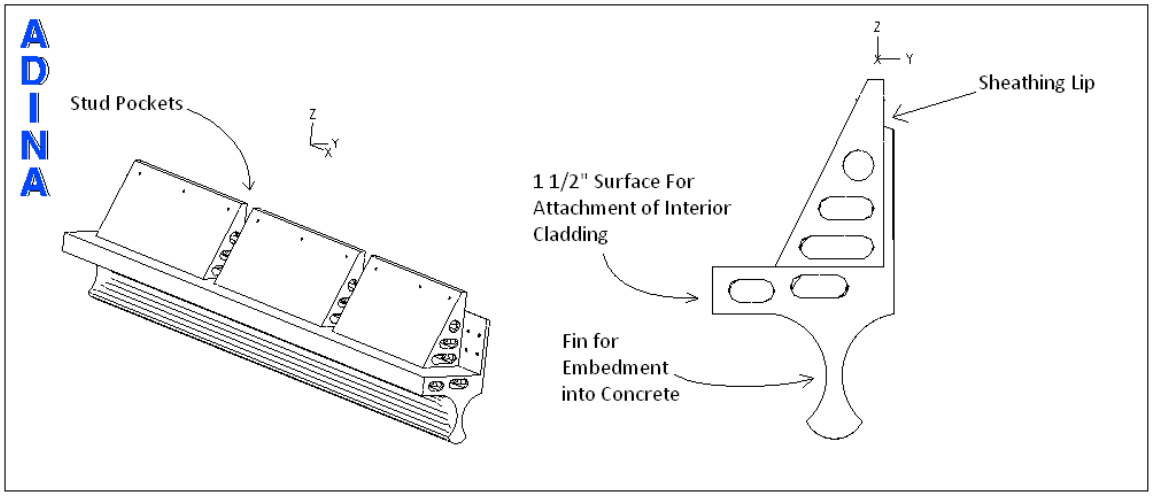

Figure 2. 1: Original Concept WPC Sill Plate

The fin on the bottom of the sill plate was the main feature of this cross-section under investigation, with hopes being that embedment of this fin into concrete would reduce bending demand on the sill plate and increase the overall strength of the shear wall. In addition to this fin, other features incorporated into the sill plate are the sheathing lip at the top and the stud pockets along the length of the sill plate. The section will be extruded as a single shape and the stud pockets will have to be routed out after cooling. The sill plate can be shipped from the manufacturer with stud pockets cut at standard 16 and 24 inch on center spacing. Non-standard spaced pockets (door and window locations, etc.) can be routed out on the job-site. The sheathing lip at the top is for attachment of the sheathing, which will act as blocking and also hold the sheathing flush with the outside to accommodate siding. The height of the section serves two purposes, first to act as flashing and protect the studs and sheathing from moisture

damage, and second, it will allow for the stud pockets which allow for side grain nailing of the studs to the sill plate eliminating a weak link in typical light-frame wood walls.

The cross-section shown in Figure 2.1 is for use with 2X6 nominal lumber. If 2X4 nominal lumber is to be used, either the section can be extruded without the flat portion at the front of the section or this portion can be cut off at the job-site.

Due to the expense associated with WPC extrusion dies, verification of the continuous anchorage concept was in order before production of the idealized sill plate was to be undertaken. Therefore, a proof of concept sill plate was manufactured and tested. The sill plate configuration tested was constructed using standard rectangular deck board cross-sections and hot-melt bonding technologies. Testing of this alternate configuration was conducted by Ross (2008), and the results are discussed in Chapter 4. The configuration tested by Ross is shown in Figure 2.2.

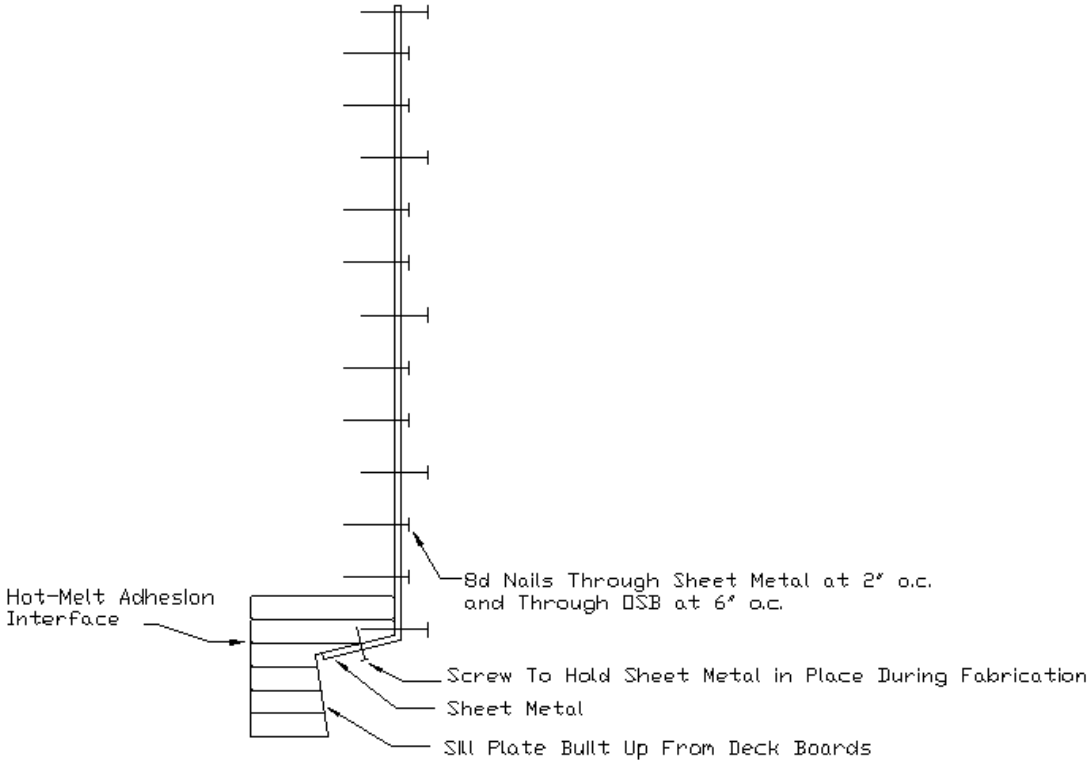

Figure 2. 2: Cross-Sectional View of Verification Sill Plate Specimen

This section was constructed by melt-bonding 1"X5.5" WPC deck boards to build up the section and then machining it to provide the fin to be embedded in concrete. The sheet metal was used to simulate the stud pockets in the original concept section.

The finite element model for both the idealized and the verification sill plates were constructed in ADINA. The verification sill plate model was comprised solely of the WPC material, the sheet metal was not included. This was done because the stress in the sheet metal is not of interest in this investigation. This project is concerned with the strength of WPC sill plates. The sheet metal is only present because it simulates the stud pockets in the verification testing as discussed above. Instead, the sheet metal is included in the wall framing model and the forces in the sheet metal-to-sill plate connectors were used to link the two models together. Also, the model does not include the hot-melt adhesion interfaces in the sill plate. The adhesion interfaces were not included in the model because the performance of hot-melt bonded WPCs was not anticipated as a failure mechanism interest in this investigation. Past research has also shown that there is a minimal drop in shear properties of hot-melt bonded WPCs (Adcock 2001b). Also, the major stress component on the melt-bonded surfaces in Ross's experimental configuration was tension perpendicular to the bond surface due to uplift forces associated with overturning action of the shear walls. Bonding of deck boards was used because a solid section of the size needed for verification sill plate manufacture was not available. In addition, the testing and inclusion of such interface properties would not have been cost-effective for the purposes of this investigation. The verification sill plate

model only serves the purpose of validating the original concept sill plate model because it can be compared against physical testing results.

As can be seen in Figure 2.2, there is a row of nails and a row of screws that attach the sheet metal to the WPC. These points were used as the load application points in the sill plate model. Similarly, loads were applied at points of nailed connections in the idealized sill plate model. The values of these loads are from the wall framing model discussed in Section 2.2.

Because only the WPC is modeled, the boundary conditions in this model simulate the interaction between the sill plate and the foundation. It was assumed that concrete foundations have enough stiffness that they will only deform a negligible amount under the loads expected to be transferred by the shear wall. Because the focus of this investigation is on the WPC, it was also assumed (and forced) that failure would occur in the sill plate, not the foundation. Because of the bulbous shape (upside-down triangular shape on the verification model) of the fin, the fin will provide bearing on the concrete in uplift. This assumption was justified by noting that the amount of material used in the cross section of the sill plate is small and therefore the horizontal strain without failure would not be sufficient to compress the sill plate enough to slide out of the concrete. By this reasoning, it was decided to model the boundary conditions of the sill plate model as bearing on a rigid body. A visual representation of this boundary condition is shown in Figure 2.3. In ADINA, the arrows pointing into the sill plate indicate the sill plate bearing on the rigid body (i.e., concrete). The arrows pointing away from the sill plate indicate the rigid body bearing on the sill plate.

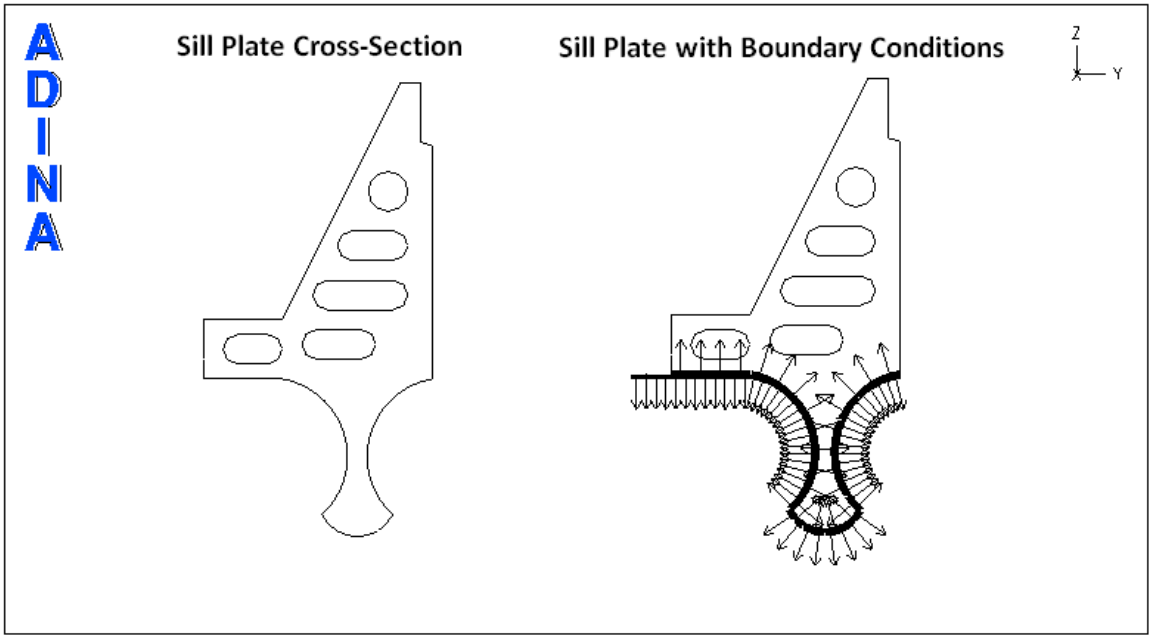

Figure 2. 3: Boundary Conditions on Sill Plate Model

To model the WPC material, 3D solid elements were utilized. The choice of using solid elements over a beam element was due to the fact that since forces will be transferred through the sill plate by means of shear and tension/compression the assumptions with which beam elements are derived do not hold up for this application (primarily the assumptions of no shear deformation and no stress perpendicular to the beam axis). Solid elements allow for all deformations/stresses to be accounted for.

WPCs are manufactured by extrusion of a molten mixture through a die. Because of this, WPC products tend to display an orthotropic material behavior due to the flow characteristics within the extruder and the cooling process (Lu 2002). To have an idealized orthotropic WPC, the material must be stranded during manufacture. Since the actual WPC material to be utilized for the idealized sill plate was unknown, it was chosen to define the material properties as being orthotropic. For the 2D model, an orthotropic material definition is not necessary because the properties in the plane of the cross-

section are the same regardless of direction. It is the out-of-plane material properties that require an alternate definition. The FE program will simply treat the 2D case as an isotropic material since the 2D case was analyzed as plane stress and the out-of-plane Poisson ratio has no effect on the in-plane results. The values of elastic modulus, and shear modulus used in the material definition of this model were obtained from Hermanson (2001a). The value used for Poisson's ratio was taken from Englund (2007).

A visual representation of the model is shown in Figure 2.4. The arrows along the length of the sill plate represent the load definitions. The block represents the foundation that is modeled as a rigid body for boundary condition purposes. Visual representation of boundary conditions have been omitted for clarity as rigid body bearing fills the image with arrows and obstructs view of most everything else.

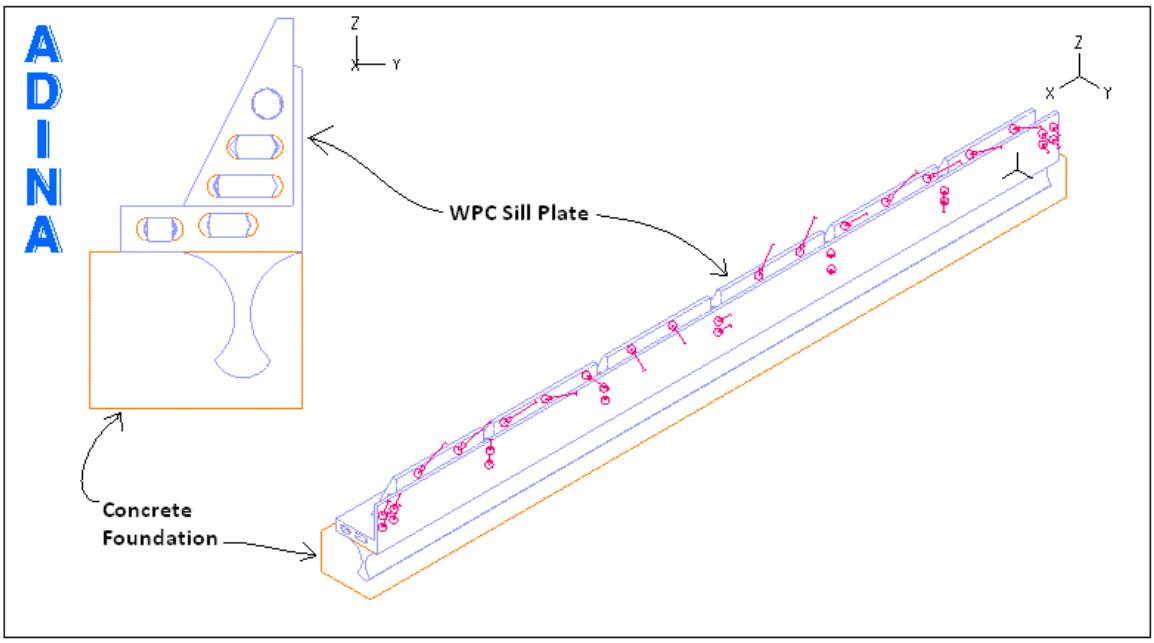

Figure 2. 4: Sill Plate Finite Element Model

The results of this analysis are presented in Chapter 4.

2.2 Wall Framing Model

2.2.1 Original Concept Wall Framing Model

The purpose of the wall framing model is to evaluate a wall under cyclic loading and predict the forces in the framing-to-sill plate and sheathing-to-sill plate connectors so that accurate loads can be applied to the sill plate model. The basis of this model is the finite element model created by Xu (2006) to test his hysteretic connector element. Xu's model was altered in the following respects:

1) The wall was extended to be eight feet long instead of four feet.
2) Because two sheathing components will be needed for an eight-foot wall, bearing in between sheets was added.
3) The sill plate was removed and all sheathing-to-sill plate connectors and stud-to-sill plate connectors were instead attached to fixed nodes that represent specific locations on the sill plate.
4) The hold-downs at the lower corners of the wall were removed.

The purpose of each change is discussed below.

The wall was made longer because most cyclic shear wall tests are done utilizing 8'X8' specimens. To check the validity of using the WPC sill plate embedded in concrete, these are the tests against which this analysis needs to be compared.

The extra sheathing component was added because OSB products are most readily available in 4'X8' sheets, and this is what is used in common construction practice. Thus, two sheets were used for an eight-foot long wall.

The sill plate was removed and modeled separately in order to be more detailed. A detailed sill plate in the framing model required more memory and processing power

than the average personal computer typically has, and the sill plate is the focus of this research and must be looked at in detail. Instead the sill plate was represented by fixed nodes that the wall framing model was attached to through the different types of connector elements discussed below. This boundary condition was justified with two assumptions: 1) because the sill plate cross section is small, strains are assumed small and 2) because the fin of the sill plate is embedded in concrete, the shear wall has continuous anchorage and bending is eliminated. These two assumptions remove the flexibility from the sill plate, allowing the sill plate to transfer forces by means of shear and tension/compression only. In addition, forces are transferred between the wall and sill plate strictly through the nail connectors. This allows the wall framing model to be attached to fixed points rather than a flexible sill plate because the sill plate will simply transfer the forces from the connectors to the foundation with only negligible deformations.

The hold-downs were removed from the wall because one of the goals of the use of a WPC sill plate embedded in concrete is to reduce the amount of hardware that need be installed.

The model was composed of 4 types of elements: beam, shell, spring, and user defined. The user defined element was developed by Xu (2006) to simulate the hysteretic connections of shear walls. The lumber was modeled with six-degree-of-freedom beam elements. The OSB was modeled with shell elements. Spring elements were utilized for the lumber-to-lumber connectors and sheathing-to-sheathing bearing elements. All other connectors were modeled with the user defined hysteretic connector element developed by Xu (2006) and modified by the author to allow different connection types in the same

model (ex. OSB-to-lumber, OSB-to-WPC, etc.). This was necessary because each type of connection behaves differently and is uniquely described by the 13 parameters which come from testing of single connections as mentioned in Section 1.2.2 (this will be discussed further in Chapter 3).

Figure 2.5 shows a side view of the model. In this figure, framing is denoted by the color brown and sheathing is denoted by the color yellow. The different types of connectors are denoted by various colors. The green connectors are non-linear springs that model the nails connecting the studs to the top plate. The red connectors are hysteretic springs that model the nails connecting the sheathing to the studs. The blue connectors are hysteretic springs that model the nails connecting the sheathing to the sill plate. The orange connectors are hysteretic springs that model the nails connecting the studs to the sill plate. Not shown are non-linear springs that model the bearing between component surfaces (i.e, between the two sheets of OSB). Hysteretic springs act in both the vertical plane and the plane into the page. All other springs only act in the direction shown. The top of the studs and the bottom of the studs were coupled to the top plate and the sill plate nodes respectively in the horizontal plane and the plane into the page.

The largest obstacle that had to be overcome with this model was the highly non-linear response of the hysteretic connectors. Non-linear problems require significantly more computer power to solve and are less likely to reach convergence. Because of the hysteretic connection behavior, the wall framing model analysis became a non-linear problem. As the simulation approached the failure load, the solution of the mathematical equations became unstable and singular, which is similar to what happens when finite elements are used to predict buckling instabilities.

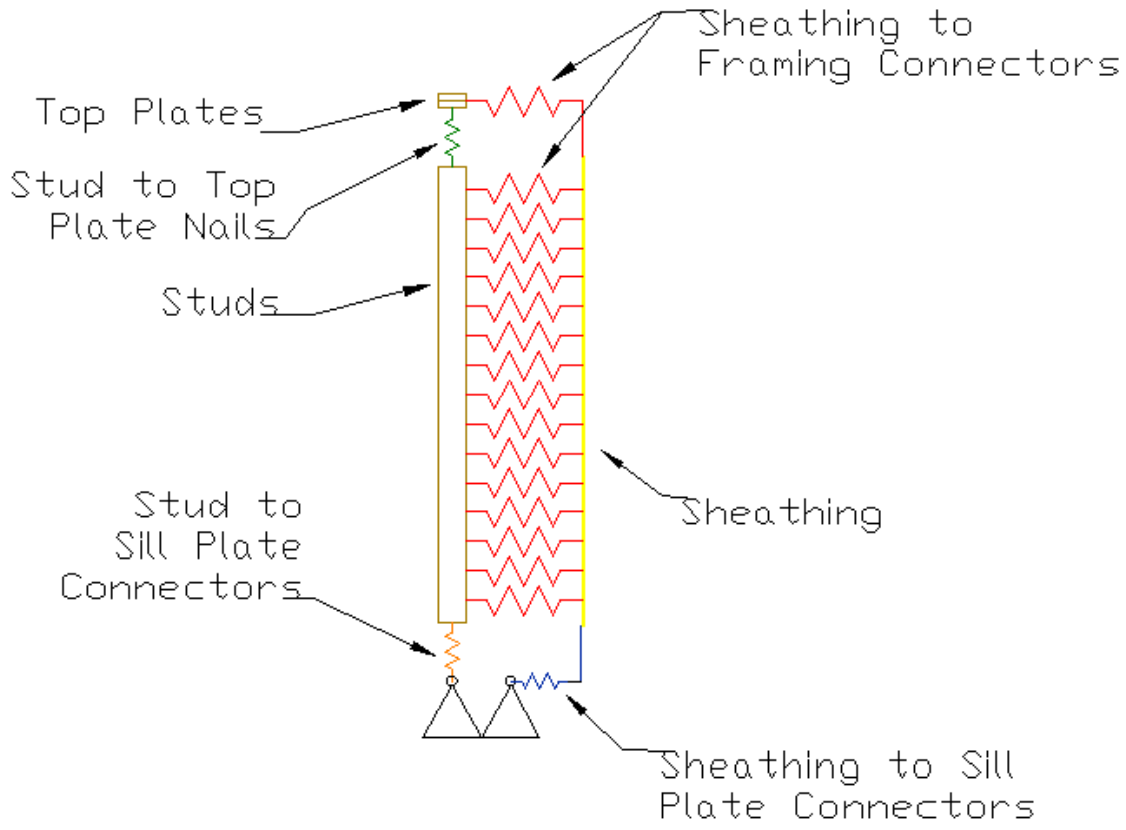

Figure 2. 5: Side View Representation of Finite Element Model

As discussed in Section 1.2.1, connector behavior is the factor that contributes most to overall shear wall performance. Each connector element affects the stiffness of the shear wall, which affects the distribution of load to all the other connectors, which in turn affects the behavior of each connector, and this circle continues. The model converges when each connector agrees on a solution and the cycle is stopped. But, because each connector is so dependent on the behavior of other connectors in this circle, and each connector has such a highly non-linear response, convergence is slow. When the hold-downs were removed from Xu's model, convergence became impossible within a reasonable amount of modeling and computer effort. After some diagnostic work, it was discovered that under the deflections that were expected, as long as only a couple of

connectors were used, the model would converge. But, with the number of connectors needed for a shear wall built to building code minimum, the solution would not converge due to the connector element's highly non-linear behavior causing endless looping of the solution in the region of large connector stiffness changes. Other methods had to be utilized to achieve a solution.

Convergence was achieved through two methods; artificial damping for most cases and a line search algorithm for cases where convergence was reached too slowly. Artificial damping is the addition of a small viscous damping effect to the hysteretic springs. The use of viscous forces works well in this model because the analysis was quasi-static. Since viscous damping is based on velocity, the damping does not affect the overall model significantly. But when a local instability occurs, the velocity increases in that region only. This allows the viscous damping forces to increase at the local instability only, keeping the model from diverging because of one connector. By adding these damping forces, the interaction of one connector with another was reduced in each step of the solution in order that the collection of connectors was capable of reaching convergence.

A line search algorithm was used when the solution diverges in early iterations using the Newton method of solution that ABAQUS uses by default. The line search algorithm makes the Newton method more robust by scaling down the residual vectors so that the correction vectors do not overshoot the solution, allowing convergence to be reached faster.

Failure of the wall framing was assumed to occur when the model could not converge on a solution for a particular step. The cause of this inability to converge was

due to negative Eigen values in the stiffness matrix. Negative Eigen values indicate a negative stiffness. Negative stiffness indicates free body motion (i.e., an unstable structure).

2.2.2 Verification Wall Framing Model

Once the original concept wall framing model was able to converge, it was altered to depict the shear wall construction utilized for the verification sill plate discussed above.

The finite element model was modified to match these verification tests by making the following changes.

1) Shell elements were added to model the sheet metal between the sheathing and framing.
2) A connection element, modeled after the bending stiffness of the cantilever portion of the sill plate cross section, was used to attach the sheet metal to the sill plate nodes.
3) Stud to sill plate connection elements were removed and replaced with bearing elements.

These changes are illustrated in Figure 2.6. The purpose of each change is discussed below.

As discussed in Section 2.1, the sheet metal elements were added because the verification tests used sheet metal instead of the originally intended stud pockets.

The purpose of the connection modeled after the bending stiffness of the cantilever portion of the cross section was an attempt to more accurately model the

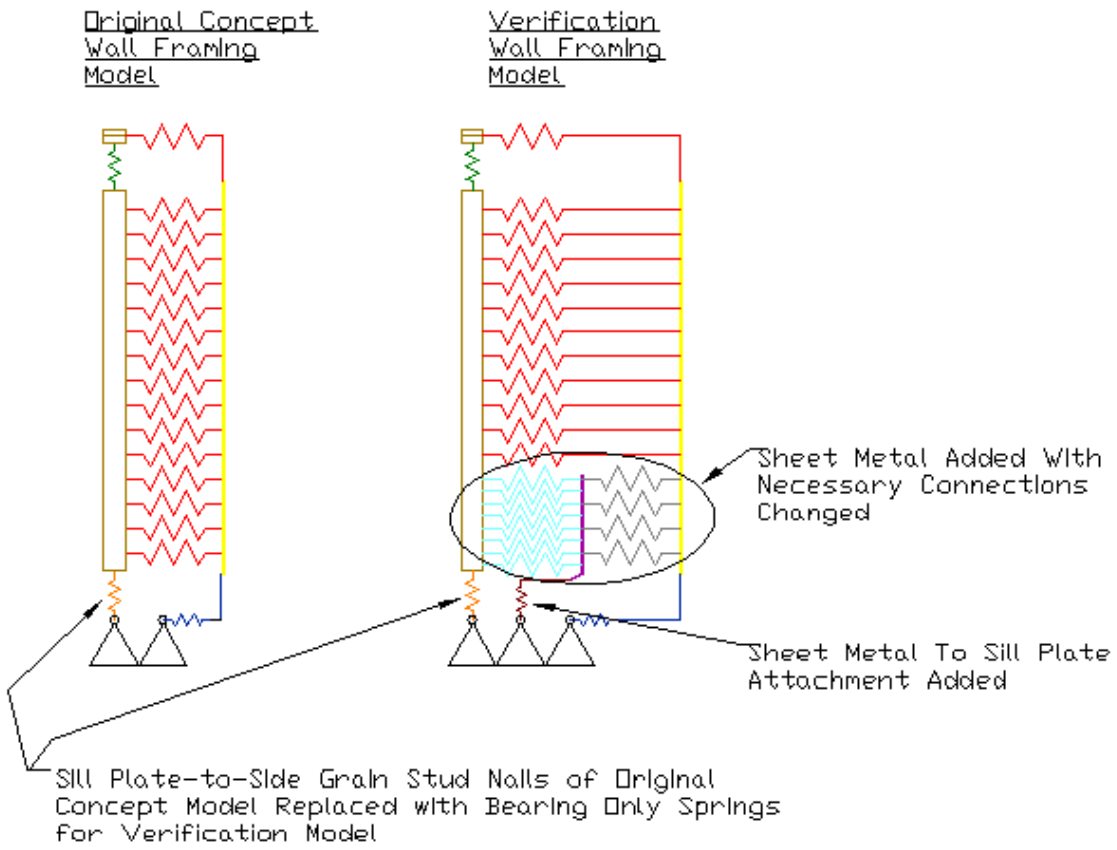

Figure 2. 6: Changes Made to the Original Concept Wall Model to Simulate the Verification Wall Configuration

specimens. Since all loads transferred to the WPC sill plate must pass through the sheet metal, the bending stiffness of the short segment between the fin embedded in the concrete and the edge where the sheathing is attached to the sill plate will play a role in distribution of forces and the performance of the shear wall. The idealized wall framing model does not incorporate this bending stiffness because the idealized sill plate is much taller and will not act as a cantilever, but the verification sill plate is short and will act as a cantilever.

The stud-to-sill plate connection elements were removed because the construction of the verification tests did not allow for a direct connection of the studs to the sill plate. However, the studs will still bear on the sill plate when compression is induced in the studs.

A side view of the verification model is shown in Figure 2.7. The purple element is the sheet metal that was added to simulate the stud pockets. The gray and turquoise connectors are hysteretic springs that model the nail behavior between the OSB and sheet metal and between the sheet metal and studs respectively. The dark brown connectors are hysteretic springs that model the bending behavior of the cantilever section of the sill plate. In this model, the orange connectors are now non-linear springs that model bearing of the studs.

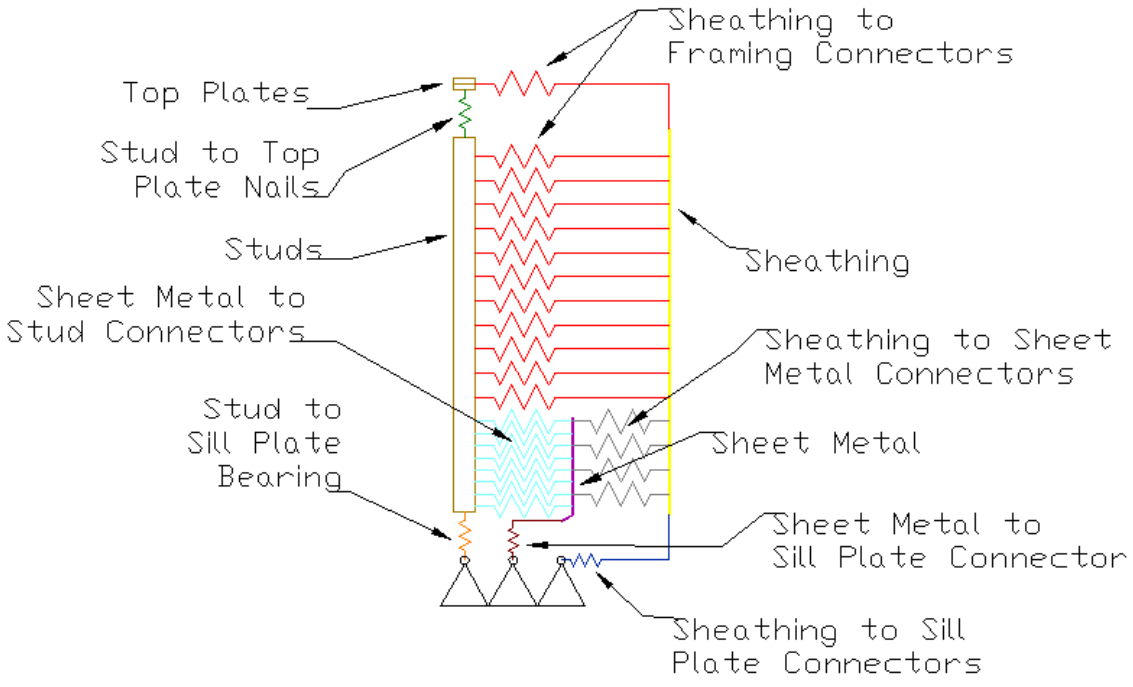

Figure 2. 7: Side View Representation of Verification Finite Element Model

CHAPTER 3: CONNECTION PERFORMANCE EVALUATION

Because the use of WPCs in conjunction with wood lumber in structural applications is a fairly new practice, the behavior of the two materials acting together is not well studied. Therefore, to develop an accurate finite element model it is necessary to first investigate the hysteretic behavior of the connections that are intended to be utilized in this application.

There are two types of connections that will be used at wood/WPC interfaces in the application being considered in this research. The first will be the connection of the WPC sill plate to the studs, the second will be the connection of the sheathing to the WPC sill plate. In addition to these, two additional connections were investigated for purposes of the verification testing, Sheet metal to lumber and OSB to lumber with sheet metal sandwiched in between.

3.1 Materials and Methods

A high density poly-ethylene (HDPE) material was used for the composite material in this research. It was chosen for two reasons; 1) it is an economical mixture in regards to price and availability and 2) it is one of the more ductile of the economical options. The higher ductility is advantageous because it reduces brittle failures and splitting due to nailing.

The sheathing used was 7/16" oriented strand board (OSB) because it is one of the most common sheathing types used in light-frame construction.

The nails used were 8d (0.131" diameter by 2 .5" long) bright box to attached sheathing to framing and 16d (0.162" diameter by 3.5" long) bright box to connect framing members. Box nails were used because they have the smallest diameter of the readily available nails and thus are assumed to be the weakest-case-scenario. Box nails are also the most common nail type used in pneumatic nailing tools.

The connection tests were conducted by attaching two pieces of material together with a nail and subjecting the assembly to cyclic loading. This was accomplished by clamping one member to the base of the testing frame while the other member is clamped to a hydraulic actuator. The actuator was driven with a cyclic displacement protocol. A schematic of the test configuration is shown in Figure 3.1.

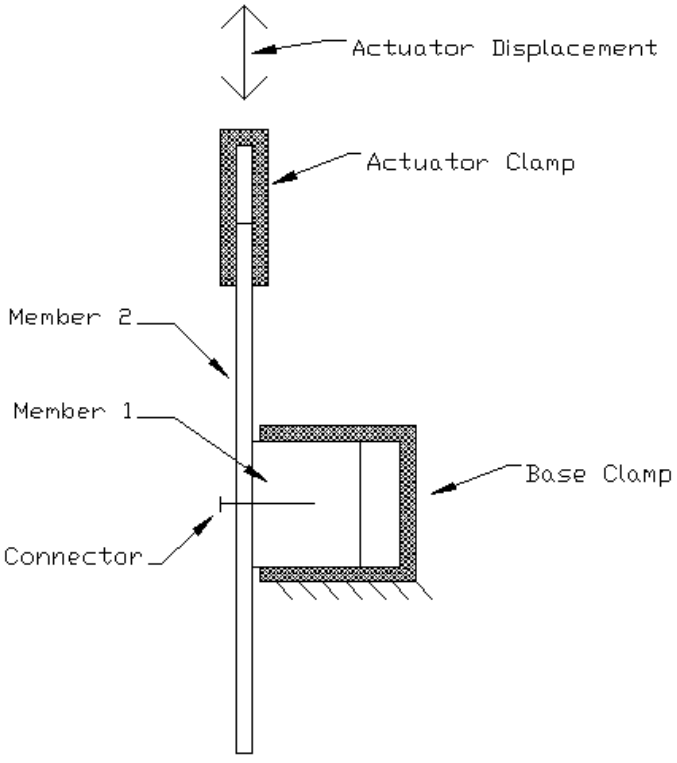

Figure 3. 1: Schematic of Testing Configuration

The testing setup is shown in Figures 3.2 and 3.3. An 11 kip actuator, MTS Model Number 244.21, was used to provide the displacement for the testing. A 3 kip force transducer type load cell, Interface Model Number SSM-AF-3000, was used to measure the load data. Displacement data was taken from the actuator displacement transducer. The testing control and data collection was accomplished using an MTS Flex Test SE controller, running Version 4.0C software. The cyclic protocol used was the CUREE basic load protocol as outlined in ASTM E2126-05.

Figure 3. 2: Test Setup

Figure 3. 3: Testing Fixture

Five types of specimens were fabricated for investigation, two of which were solely for the purposes of the proof of concept testing. The different specimen configurations are presented out in Table 3.1 and are shown in Figures 3.5 to 3.7. After assembly, the specimens were conditioned at 70 ºF and 65% relative humidity for two weeks.

Table 3. 1: Connection Specimens

Member 1	Member 2	Nail Size	Number of Nails
7/16" OSB	WPC	8d	1
3/8" WPC	#2 DF(N) wood lumber	16d	1
3/8" WPC	#2 DF(N) wood lumber	16d	2
Sheet Metal	#2 DF(N) wood lumber	8d	1
7/16" OSB	Sheet Metal	8d	1

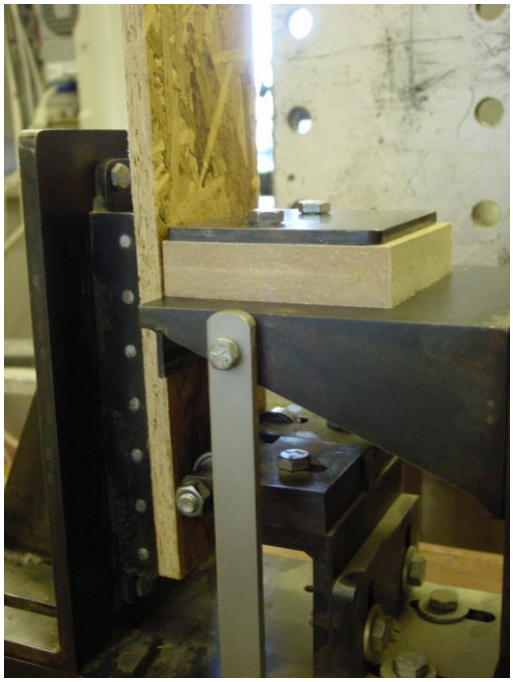

Figure 3. 4: OSB Connected to WPC With an 8d Nail

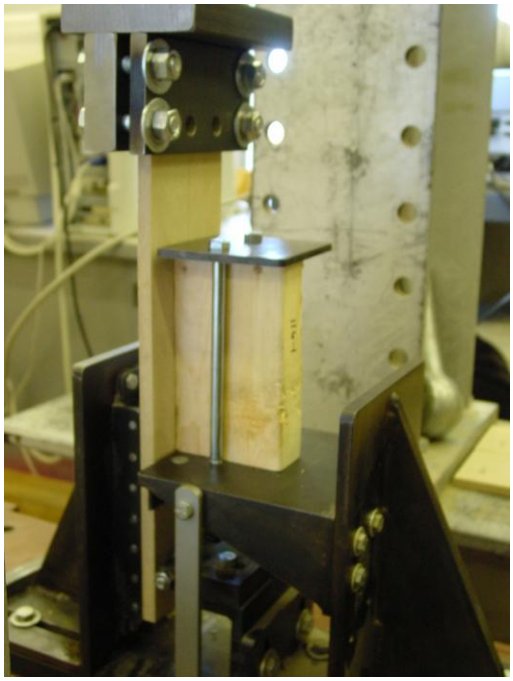

Figure 3. 5: WPC Connected to Lumber With a 16d Nail

Figure 3. 6: Sheet Metal Connected to Lumber With an 8d Nail

Figure 3. 7: OSB Connected to Lumber With an 8d Nail Through Sheet Metal

3.2 Results

Since the goal of this research was to develop a finite element model in order to investigate the performance of WPC sill plate configurations, the results sought were the necessary parameters to model the hysteretic behavior of the nailed connections. It has been shown that hysteretic nail behavior can be modeled accurately using 13 parameters that can be obtained from cyclic connection tests (Xu 2006). These 13 parameters describe such things as stiffness, hardening, degradation rate, rate of change of force/displacement curve, etc. and are discussed further by Xu (2006). The parameters obtained from fitting the hysteretic model to the test data are presented in Table 3.2.

Table 3. 2: Average Hysteretic Parameters Determined From Connection Test Data

Parameter	8d OSB to WPC	16d WPC to Lumber	(2) 16d WPC to Lumber	8d Sheet Metal to Lumber	8d OSB to Lumber Sandwiching Sheet Metal
α	0.027840	0.020025	0.058145	0.021070	0.021420
β	2.166664	1.794860	1.685328	1.800845	2.019187
ω	1.197318	1.177060	1.199904	1.193378	1.149249
ζ_0	0.955104	0.969288	0.968549	0.965943	0.960158
n	1.208475	1.052120	1.002695	1.015015	1.030783
ψ	0.193183	0.331871	0.115241	0.163206	0.249759
δ_ψ	0.082974	0.035277	0.058654	0.089015	0.072605
δ_ν	0.001445	0.007939	0.000008	0.006970	0.003092
ξ	0.000014	0.000015	0.000013	0.000014	0.000013
γ	-1.186347	-1.258440	-1.185000	-1.274032	-1.267470
δ_η	0.007693	0.009902	0.002843	0.007988	0.006978
p	1.438957	1.050055	0.939987	1.570365	1.413761
q	0.132933	0.143762	0.196777	0.083840	0.113750

The values in the table above were obtained by processing the test data using the genetic algorithm described by Heine (2001). In short, the genetic algorithm starts with an assumed value for each parameter, changes the value by a small percentage and checks the fit of each set of parameters to the data. The set of parameters that most closely produces a force/displacement curve resembling that obtained from the test data is considered "more fit" for the job. Next, the values are modified in such a way that imitates genetic refinement seen in biological organisms (i.e., genetic mutation and natural selection). The process is repeated until the parameters yield results within a specified accuracy using a least value of the square root of the sum of the squares of error approach. Each test's data was run through the algorithm to obtain the 13 parameters for individual tests. The values used in the FE model (those in the table above) are the average of values for tests of a particular connection configuration. The parameters obtained have coefficients of variation ranging from 1% to 30% typically, with a few outliers as high as 59%.

CHAPTER 4: VERIFICATION AND SIMULATIONS

4.1 Evaluation Parameters

There are several parameters that must be considered when evaluating shear wall performance under cyclic loading.

The first of these parameters is the shear strength. This is the value that is typically published in design manuals and is the structural engineer's primary deciding factor when designing a shear wall. The shear strength is calculated as the peak load distributed over the length of the shear wall (i.e., strength per unit length). Mathematically, the shear strength is defined as:

$$v = \frac{P_{peak}}{L} \tag{4.1}$$

where P_{peak} is the maximum absolute load that the shear wall experienced during testing and L is the length of the shear wall.

To estimate of shear wall stiffness when subjected to multiple loading cycles, the elastic shear stiffness is used. The elastic shear stiffness is defined as the slope of the equivalent energy elastic-plastic (EEEP) curve. The EEEP curve is an idealized elastic-plastic curve in which the area under the curve is equal to the area under the hysteretic backbone curve. Development of an EEEP curve is outlined in ASTM E 2126-05 (2005). The elastic shear stiffness is expressed as:

$$K_e = \frac{0.40 P_{peak}}{\Delta_e} \tag{4.2}$$

where Δ_e is the displacement along the EEEP curve at 40% of the peak load.

Ductility is a measure of inelastic deformation before failure. Ductility is important in a structure because it gives some warning before failure, allowing people to safely exit the structure before it collapses. Also, the more ductile a component is the less force it will attract and less chance that failure loads will be reached. Ductility is expressed as:

$$D = \frac{\Delta_u}{\Delta_y} \tag{4.3}$$

where Δ_u and Δ_y are displacements at ultimate load and yield respectively. The yield displacement is taken from the EEEP curve.

Another important factor in shear wall evaluation under cyclic loading is the amount of seismic energy that can be dissipated by the shear wall. Dissipated energy is the area enclosed by the hysteretic loops of the force-displacement curve.

4.2 Model Verification

To verify the accuracy of the continuous anchorage finite element model developed in this thesis, verification tests of a similar sill plate configuration were conducted and the model modified to match the parameters of those tests. This section contains the results of those tests.

4.2.1 Verification Testing Results

The results in this section are from shear wall tests conducted by Ross (2008). Ross conducted shear wall tests utilizing the verification sill plate configuration discussed in Chapter 2. However, due to problems that occurred during data acquisition, the results

cannot be used for a meaningful numerical analysis. The discussion in this chapter concerning the verification testing will be strictly of a qualitative nature.

Only one specimen from the verification testing was chosen to consider as a comparison for the model because it was the only specimen that yielded usable data. The results of this test are shown in Figure 4.1. This test had a peak load of 34.96kN (7860lb) which occurred at a displacement of 22.1mm (0.871 in). As can be seen in the figure, the data is very "choppy". This choppiness was caused by a data recording frequency that was too slow. The wall had a maximum displacement of 36.7mm (1.44 in) before failure.

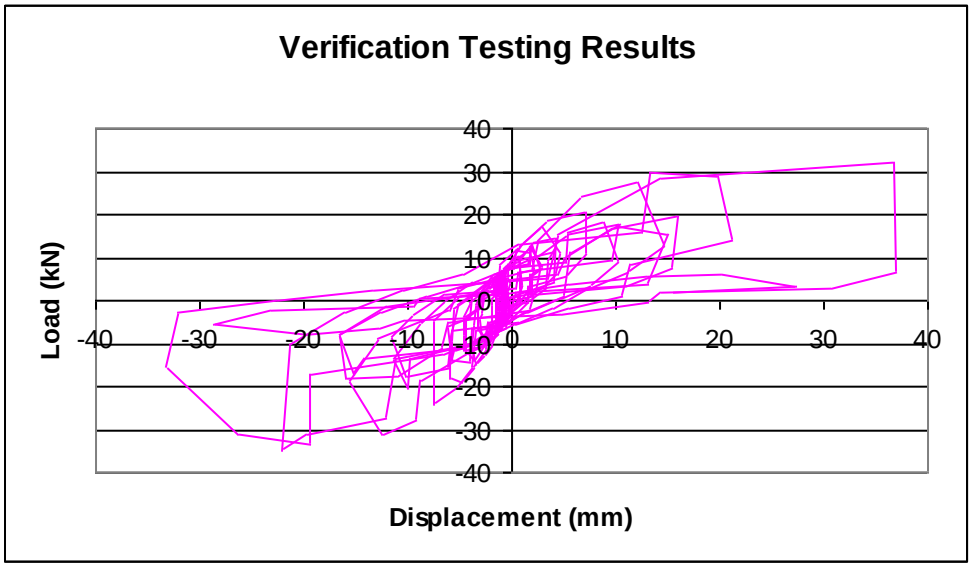

Figure 4. 1: Verification Test Results

4.2.2 Verification Model Results

The wall framing model was run using the same CUREE basic loading protocol that was used in the verification tests. The model yielded a peak load of 30.87kN (6940lb) at a displacement of 17.8mm (0.701in). The model results are shown in Figure 4.2.

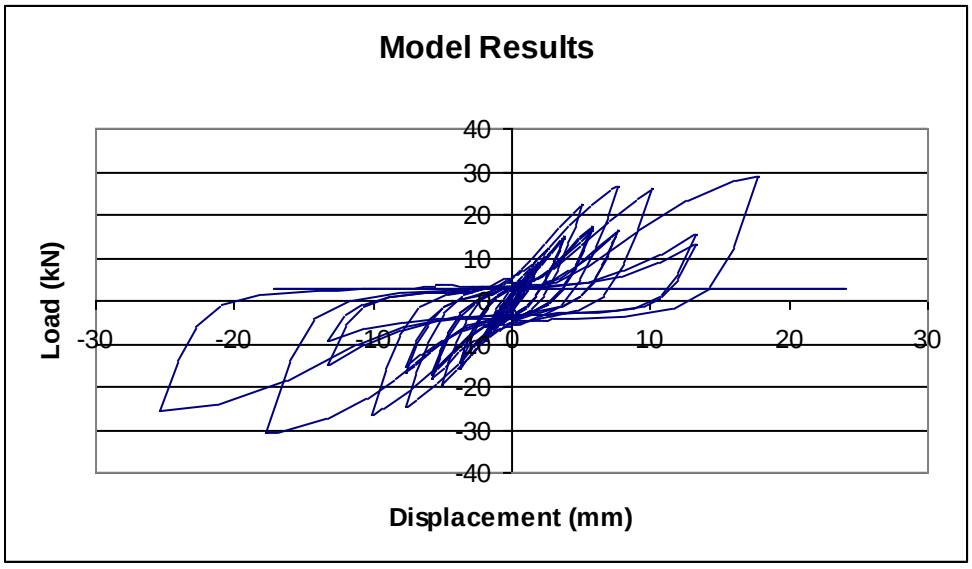

Figure 4. 2: Verification Wall Framing Model Results

4.2.3 Comparison of Verification Model to Testing Results

The finite element model outputs and the verification testing data are plotted together in Figure 4.3.

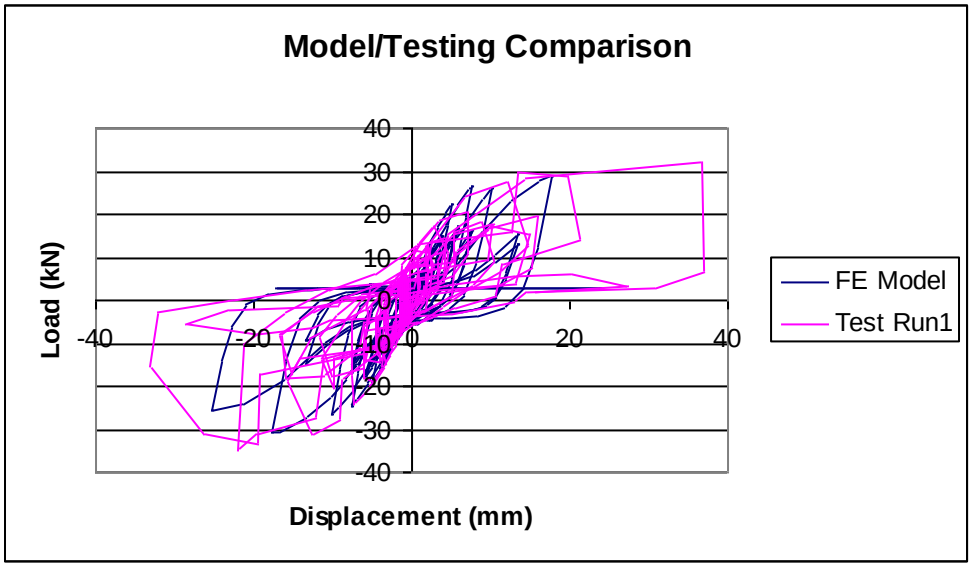

Figure 4. 3: Model Results Superimposed with Verification Test Data

As can be seen in the figure above, the model results follow the test data backbone curve fairly accurately in the early stages of the testing. However, the model does predict an earlier failure of the wall than that which occurred during testing. This was due to problems that occurred during manufacture of the verification sill plate which resulted in a sill plate that displayed a more ductile behavior than that which was modeled. The main cause of the increased ductility in the test wall was due to a weak melt-bond adhesion at the critical section of the sill plate. Melt-bonding is accomplished by heating up two pieces of WPC and pressing them together, infusing the two soft surfaces. During specimen manufacture for the verification testing, deck boards were positioned under heat lamps as shown in Figure 4.4. Because there is such a narrow range of temperatures that are effective in melt-bonding WPCs, only the area directly under the heat lamps adhered properly. The critical sections of the sill plate are at the ends of the member, and did not adhere properly. This reduced the capacity of the wall to resist overturning moment, resulting in a greater deflection of the wall. In regards to overturning restraint, the lack of proper adhesion at the ends could be likened to reducing the length of the shear wall. Although the verification test did have an increase in deflection, the peak load remained similar to that predicted by the model.

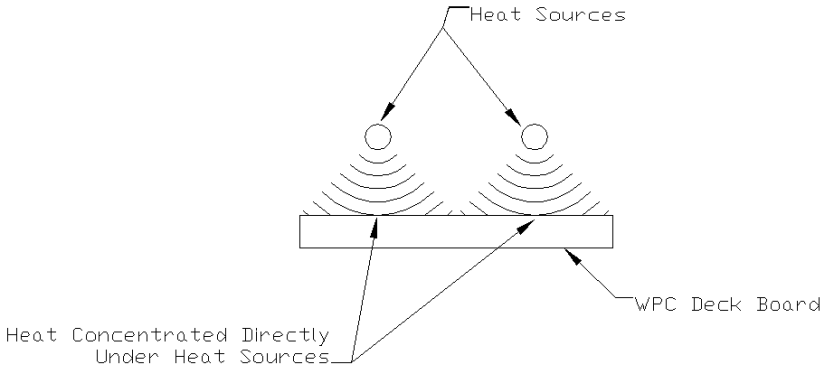

Figure 4. 4: Manufacture of Verification Sill Plates

4.3 Continuous Anchorage Shear Wall Simulation

The sill plate model was analyzed as both a 3-D solid model and a 2-D plane stress model. Plane stress was chosen over plane strain because the critical sections of the sill plate are at the ends of the member (this was verified by the 3-D model), where plane stress would be a more accurate representation than plane strain. Principal stress was chosen as the rupture criterion because the mode of failure for a WPC material under these circumstances is tension perpendicular to extrusion. At the same time, WPCs exhibit a somewhat brittle failure tendency, which makes principal stresses a good failure criterion for the material. The wall framing model was run as a 3-D model fixed against out-of-plane motion.

4.3.1 Original Concept Model Results

The idealized wall framing model predicts a maximum load of 24.1kN (5418 lb) at a displacement of 62.3mm (2.45 in). When this peak load occurred, the idealized sill plate model predicted a principal stress of 6.9MPa (1000psi). This is under the rupture strength perpendicular to extrusion of HDPE, which is 10.3MPa (1500psi) (Hermanson 2001a). Since the peak load from the wall framing model does not cause the sill plate to reach failure, failure is predicted to occur in the framing (i.e., sheathing-to-framing connections) before the sill plate fails.

The results of the sill plate 3-D and 2-D analyses were within 10% of each other and can be seen in Figure 4.5 and 4.6 respectively. At first glance of these figures, it appears that there are some stresses that are higher than where the peak stress is indicated

(i.e., the red areas). These are actually due to computer interpretation and can be ignored. These areas appear to have higher stress than they actually do because these are the points of load application (the red arrows indicate points of load application). Because loads were applied to the model as point loads, the computer interprets them as concentrated at a single point on the specimen. Because a single point has essentially no area, the stresses are depicted a lot higher than they actually are at these locations.

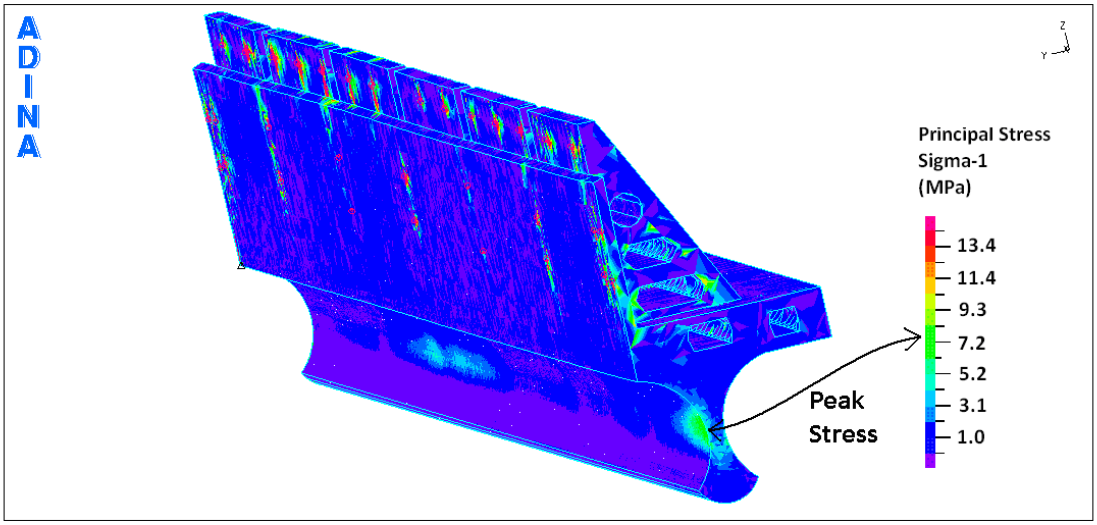

Figure 4. 5: 3-D Stress Analysis Results

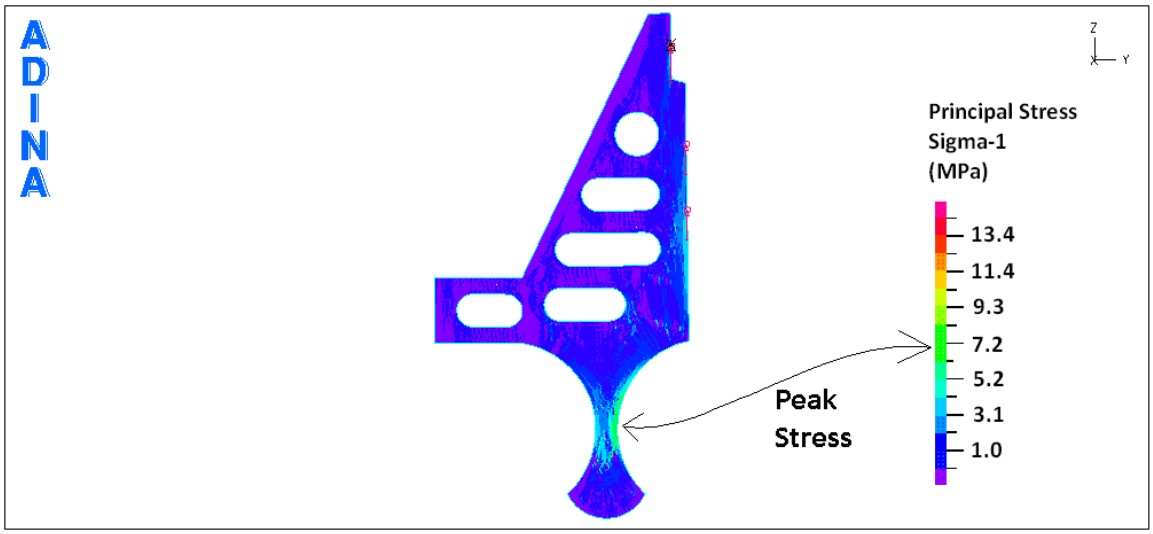

Figure 4. 6: 2-D Plane Stress Analysis Results

4.3.2 Comparison of Original Concept Model with Other Wall Configurations

The results of the idealized model were compared to four past cyclic shear wall tests in order to assess the performance of the continuous anchorage WPC sill plate in relation to other configurations. To compare with shear walls built using typical construction practices, the model results were compared against shear wall results utilizing 2X4 (from Salenikovich 2000) and 2X6 (from Duchateau 2005) nominal wood sill plates. To compare with a straight substitution WPC sill plate configuration, the model results were compared against the WPC sill plate tested by Duchateau (2005) that had pockets for the studs and provided stud rotational resistance. This was the configuration that exhibited the best performance of all her specimens. The results of these tests and the model are summarized in Table 4.1.

From Table 4.1, it can be noted that, in terms of strength, the performance of a shear wall utilizing a continuous anchorage sill plate is more than twice that of a typical unanchored shear wall and slightly better than a typical fully anchored shear wall.

When compared to Duchateau's 2005 shear wall test incorporating the WPC sill plate with stud rotational resistance, the results are a slight decrease in strength and energy dissipation. However, the continuously anchored shear wall did show an increase in ductility over the straight substitution WPC sill plate. The increase in ductility was caused by the increase in stiffness shifting the yield displacement to a lower value. The increased stiffness is due to both the continuous anchorage and the direct sheathing-to-sill plate connections incorporated in the continuously anchored shear wall.

Table 4. 1: Shear Wall Capacities of Various Configurations

	Peak Load (kN)	Ultimate Displacement (mm)	Shear Strength (kN/m)	Stiffness (kN/mm)	Ductility	Energy Dissipation[c] (kN-mm)
2X4 Nominal Wood Sill Plate with No Anchorage[a] (Salenikovich 2000)	10.8	36	4.4	1.4	5.4	3,584
2X6 Nominal Wood Sill Plate with No Anchorage[b] (Duchateau 2005)	10.8	45	4.4	1.8	8.1	2,420
2X4 Nominal Wood Sill Plate with Full Anchorage[a] (Salenikovich 2000)	19.4	73	8.0	1.9	7.6	15,079
WPC Sill Plate With Stud Rotational Resistance Tested by Duchateau[b] (2005)	28.6	77	11.7	1.2	3.6	6,398
WPC Sill Plate with Continuous Anchorage[b] (model)	24.1	64	9.9	1.5	4.7	6,059

[a] values derived from testing using Sequential Phase Displacement (SPD) Protocol
[b] values derived from testing using CUREE basic load protocol
[c] energy dissipation cannot be directly compared between SPD and CUREE protocols

Since one of the goals in this study is to investigate the effects of continuous anchorage, a closer comparison of the two configurations utilizing a WPC sill plate is warranted. The wall framing model results are superimposed with Duchateau's 2005 test results in Figure 4.7.

The shear wall with continuous anchorage and the shear wall without continuous anchorage follow a similar backbone curve trend. However, the continuously anchored shear wall loses stiffness faster and does not reach as high of a load as Duchateau's shear wall. This was due to the fact that with continuous anchorage there is no bending in the sill plate. All racking motion is accommodated by bending of the fasteners and/or

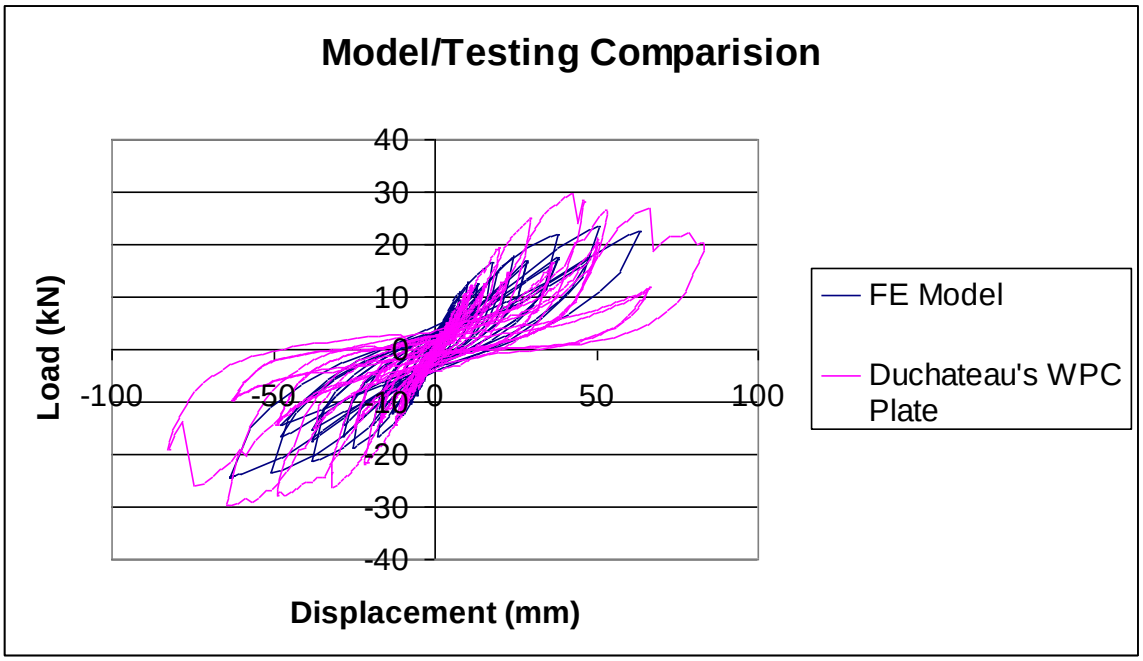

Figure 4. 7: Model Results Superimposed with Duchateau's WPC Sill Plate Test Data

deformations of the structural members. This leads to a faster rate of strength degradation, earlier fatigue of the connectors and subsequently an earlier wall failure. Also Duchateau's sill plate cross-section had twice the area of the continuous anchorage sill plate. This resulted in more restraint on the motion of the studs and subsequently a higher load capacity as the studs were capable of transferring horizontal forces through bearing and in-plane bending of the studs on the sides of the stud pockets.

To evaluate the performance of the continuous anchorage shear wall concept in the field, the model results were compared to current design codes.

The Building Seismic Safety Counsel TS-7 suggests a maximum value of 2.6kN/m (180plf) nominal when designing unrestrained light-frame wood shear walls (Dolan 2008). The FE model presented in this thesis gives a nominal value of 9.8kN/m (672plf).

From the National Design Specification (2005), the allowable shear strength of an engineered shear wall of similar nailing schedule and sheathing type to that modeled is 3.50kN/m (240plf). Taking into account a factor of safety of 2.8 for seismic, the value associated with ASD unit shear capacity for shear walls and diaphragms, the results of the FE model yield an allowable shear strength of 3.53kN/m (242plf).

The continuously anchored shear wall model was shown to be reasonably accurate. The model was used to predict the performance of a shear wall utilizing an idealized WPC sill plate. The results of the analysis were encouraging.

CHAPTER 5: CONCLUSIONS AND RECOMMENDATIONS

5.1 Conclusions

This thesis has shown that in light-frame wood shear walls, sill plate performance calls for some investigation. Past research involving investigation into light-frame wood sill plates was reviewed. This thesis contains the next step in this ongoing investigation by considering a WPC sill plate configuration that provides continuous anchorage for light-frame wood shear walls.

This thesis utilized finite element modeling to investigate the performance of a continuous anchorage WPC sill plate. The model incorporates hysteretic connection behavior at its core to accurately predict shear wall behavior. This hysteretic connection behavior was derived from testing of single connections.

Based on the finite element model developed in this thesis, continuously anchored light-frame wood shear walls show increased performance over typical shear walls in regards to capacity. The continuously anchored shear wall has an increased capacity over typical unrestrained shear walls of 230% and over typical overturning restrained shear walls of 24%.

In comparison to WPC sill plates with stud rotational resistance secured to a foundation with anchor bolts (i.e., intermittent anchorage), the continuous anchorage sill plate experienced stiffness degradation sooner resulting in a slightly lower capacity, but an increase in ductility. The capacity issue can be addressed by considering the material stiffness of the continuous anchorage sill plate.

The continuously anchored shear wall demonstrated a negligible difference (0.9%) in unit shear strength when compared alongside engineered shear walls and an increase of 277% in relation to prescriptive shear walls.

The shear wall configuration proposed in this thesis has the potential of replacing shear walls with overturning restraint and a 6/12 nailing schedule as the two are comparable in strength, but the WPC does provides additional benefits in regards to moisture related decay. The addition of the continuous anchorage reduced sill plate bending, eliminating one major mode of failure from shear walls.

5.2 Recommendations and Future Research

5.2.1 Connection Tests

Since overall shear wall performance is controlled by connector behavior, this research utilized testing of single connections in order to accurately predict shear wall behavior. The following is recommended based on the results of that testing.

- The use of equipment capable of recording velocity and acceleration of the connection test data would increase the accuracy of the 13 parameters used to model the hysteretic behavior of the connections.
- A closer look at the effects of direction of connector loading with respect to WPC extrusion direction and lumber grain direction would increase the accuracy of the hysteretic parameters.

5.2.2 Finite Element Model

To improve the accuracy of the finite element model, the following recommendations are made.

- A detailed investigation into the orthotropic properties of a chosen formulation of WPCs for the sole purpose of providing modeling data will yield a more accurate model.
- Combining the wall framing model and the sill plate model into one model will yield more accurate results. This can be accomplished in two ways.
    - If a high powered computer can be obtained, the sill plate can be modeled directly in the wall framing model.
    - More realistically, a model of the sill plate can be used to calculate the mechanical properties of the sill plate and these properties can be assigned to a general element type that can be included in the wall framing model.

5.2.3 General Recommendations

In addition to the recommendations above, a few additional items that could be investigated on their own which will further develop the usefulness and understanding gained from this thesis are:

- An investigation into basic mechanical properties of different types of WPC materials would allow for a more accurate finite element model and lead to a better choice of WPC formulation for different application. In particular,

nailability was an issue during verification testing and could be considered with an investigation into mechanical properties of WPCs.

- Investigation into the shape and size of the anchorage bulb, while taking into account the concrete strength and common construction practices, would help to maximize the effects of the continuous anchorage concept.
- An investigation into the effects of adding reinforcement to weak areas of the continuous anchorage sill plate (like the sheathing lip) would further increase the usefulness of the idealized sill plate considered in this thesis.

5.3 Closing Comments

A WPC sill plate designed to provide continuous anchorage of light-frame wood shear walls was investigated in this thesis. WPCs have been shown to be a viable alternative to the typical wood sill plate in light-frame wood shear walls. With this alternate sill plate configuration, strengths similar to those found in typical overturning restrained shear walls can be achieved without the use of added hardware, but with the added benefit of resistance to moisture related decay that WPCs can provide.

REFERENCES

Adcock, Timothy, Wolcott, Michael P., and Hermanson, John C. (2001a). " The Influence of Wood Plastic Composite Formulation: Studies on Mechanical and Physical Properties." Project End Report. Engineered Wood Composites for Navy Waterfronts. Task 1D-1 Evaluate Extruded Materials. Washington State University. Pullman, Washington.

Adcock, Timothy, Wolcott, Michael P., and Dostal, David. (2001b). " Co-Extrusion of Wood Plastic Composites: The Flexural Behavior of Capped/Foamed/Fiber Reinforced Wood Plastic Composite." Project End Report. Engineered Wood Composites for Navy Waterfronts. Task 2H Evaluate Extruded Materials. Washington State University. Pullman, Washington.

Anderson, Erin, Leichti, Robert, Sutt, Edward, and Rosowsky, David. (2006). "Sheathing Nail Bending-Yield Stress: Effect on Cyclic Performance of Wood Shear Walls." *Wood and Fiber Science*, 39(4), 536-547.

ASTM E 2126-05. (2005). "Standard Test Methods for Cyclic (Reversed) Load Test for Shear Resistance of Vertical-Elements of the Lateral-Force Resisting Systems for Buildings." American Society of Testing Materials. Vol. 04.12.

Bredel, Daniel. (2003). "Performance Capabilities of Light-Frame Shear Walls Sheathed with Long OSB Panels." Master's Thesis, Virginia Polytechnic Institute and State University, Blacksburg, VA.

CRD. (2007). "Conceptualized Reference Database for Building Envelope Research." Building Envelope Performance Laboratory, Centre for Building Studies. Department of Building civil and Environmental Engineering. Concordia University. <http://alcor.concordia.ca/~raojw/crd/index.html>

DIS. (2007). "Fact on the January 17, 1994 Northridge Earthquake." DIS, inc. Sparks Nevada. <http://www.dis-inc.com/northrid.htm>

Dolan, J. Daniel. (2008). Washington State University, Department of Civil and Environmental Engineering and member of the Building Seismic Safety Council TS-7. (personal correspondence)

Dolan, J.D. (1989). "The Dynamic Response of Timber Shear Walls." PhD Dissertation, The University of British Columbia.

Dolan, J.D., and Madsen, B. (1992). "Monotonic and Cyclic Nail Connection Tests." *Canadian Journal of Civil Engineering*, 19, 97-104.

Dowrick, D.J. (1986). "Hysteretic Loops for Timber Structures." *Bulletin of the New Zealand National Society of Earthquake Engineering*, 19(20), 143-152.

Duchateau, Kristin A. (2005). "Structural Design and Performance of Composite Wall-Foundation Connector Elements." Master Thesis, Washington State University.

Englund, Karl. (2007). Washington State University, Wood Materials and Engineering Laboratory. (personal correspondence)

Falk, R.H. and Itani, R.Y. (1989). "Finite Element Modeling of Wood Diaphragms." *Journal of Structural Engineering*, 115(3), 543-559.

Foliente, G.C. (1995). "Hysteresis Modeling of Wood Joints and Structural Systems." Journal of Structural Engineering, 121(6), 1013-1022.

Foschi, R.O. (1977). "Analysis of Wood Diaphragms and Trusses, Part One: Diaphragms." *Canadian Journal of Civil Engineering*, 4(3), 345-352.

Gutkowski, R.M. , and Castillo A.L. (1988). "Single- and Double- Sheathed Wood Shear Wall Study." *Journal of Structural Engineering*, 114(6), 1268-1284.

Heine, Christopher P. (1997). "Effects of Overturning on the Performance of Fully Sheathed and Perforated Timber Framed Shear Walls." Master's Thesis, Virginia Polytechnic Institute and State University.

Heine, Christopher P. (2001). "Simulated Response of Degrading Hysteretic Joints With Slack Behavior." PhD Dissertation, Virginia Polytechnic Institute and State University.

Hermanson, John C., Adcock, Timothy, Wolcott, and Michael P. (2001). "Evaluation of Extruded Materials: Materials Development." Project End Report. Engineered Wood Composites for Navy Waterfronts. Task 1F Evaluate Reinforced Materials and Task 1G Model Material Performance . Washington State University. Pullman, Washington.

Itani, R.Y., and Cheung, C.K. (1984). "Nonlinear Analysis of Sheathed Wood Diaphragms." *Journal of Structural Engineering*, 110(9), 2137-2147.

Kubal, Michael T. (2000). "Construction Waterproofing Handbook." McGraw Hill. New York, New York.

Lu, Guibin. (2002). "HDPE Wood-Plastic Composite Material Model Subject to Damage." Master Thesis, Washington State University.

Mahaney, James A., and Kehoe, Brian E. (2002). "Anchorage of Wood-frame Buildings: Laboratory Testing Report (CUREE Publication No. W-14)." CUREE, Richmond, CA.

McCutcheon, W.J. (1985). "Racking Deformations in Wood Sher Walls." *Journal of Structural Engineering*, 111(2), 257-269

National Design Specification (NDS). (2005). American Forest and Paper Association. AF&PA, Washington, D.C.

Pendleton, David E., Hofford, Theresa A., Adcock, Tim, and Wolcott, Michael P. (2002). "Durability of an extruded HDPE/wood composite." *Forest Products Journal*. Forest Products Society, 52(6), 21-27.

Polensek, A. (1976). "Finite Element Analysis of Wood-Stud Walls." *Journal of Structural Engineering*, 102(7), 1317-1335.

Rose, John D. (1998). "Preliminary Testing of Wood Structural Panel Shear Walls Under Cyclic (Reversed) Loading." APA Research Report 158. APA – The Engineered Wood Association, Tacoma, Washington.

Ross, Loren. (2008). "Performance of Wood Plastic Composite Foundation Elements in Post-Frame and Light-Frame Shear Walls." Master Thesis, Washington State University.

Salenikovich, Alexander. (2000). "The Racking Performance of Light-Frame Shear Walls." PhD Dissertation, Virginia Polytechnic Institute and State University.

Stewart, W.G. (1987). "The Seismic Design of Plywood Sheathed Shear Walls." PhD Dissertation, University of Canterbury.

Toothman, Adam. (2003). "Monotonic and Cyclic Performance of Light-Frame Shear Walls with Various Sheathing Materials." Master's Thesis, Virginia Polytechnic Institute and State University.

White, Maurice, Dolan, J. Daniel. (1995). "Nonlinear Shear-Wall Analysis." *Journal of Structural Engineering*, 21(11), 1629-1635.

Xu, Jian. (2006). "Development of a General Dynamic Hysteretic Light-frame Structure Model and Study on the Torsional Behavior of Open-front Light-frame structures." PhD Dissertation, Washington State University.

APPENDIX A: CONNECTION TEST RESULTS

Table A. 1: Tabulated Parameters for 8d (0.131" diameter by 2 .5" long) OSB to WPC Connections

Parameter	Test Run					
	1	2	3	4	5	6
α	0.022333	0.039312	0.020434	0.027304	0.031232	0.026427
β	1.934092	2.074452	2.419028	2.214796	2.182850	2.174768
ω	1.188793	1.198872	1.199768	1.197412	1.199942	1.199123
ζ_0	0.964965	0.958849	0.959353	0.947558	0.946536	0.953363
n	1.300810	1.306868	1.032825	1.274944	1.207652	1.127748
ψ	0.340566	0.107242	0.338610	0.135855	0.103322	0.133505
δ_ψ	0.056645	0.094341	0.050149	0.099179	0.097858	0.099672
δ_ν	0.002684	0.002539	0.000227	0.000000	0.001439	0.001782
ξ	0.000011	0.000014	0.000014	0.000014	0.000015	0.000013
Υ	-0.881459	-1.179010	-1.228343	-1.300000	-1.257506	-1.271765
δ_η	0.004101	0.009019	0.009014	0.007704	0.009390	0.006929
p	1.153258	1.564985	1.242124	1.581370	1.517753	1.574254
q	0.141454	0.153282	0.094072	0.162405	0.118745	0.127638

Table A. 2: Tabulated Parameters for 16d (0.162" diameter by 3.5" long) WPC to Lumber Connections

Parameter	Test Run						
	1	2	3	4	5	6	7
α	0.020047	0.020048	0.020063	0.020018	0.020000	0.020000	0.020000
β	1.817002	1.812859	1.724236	1.760874	1.810166	1.822605	1.816276
ω	1.182421	1.126112	1.188200	1.152213	1.199392	1.194715	1.196366
ζ_0	0.966941	0.969919	0.969927	0.969984	0.969971	0.969657	0.968619
n	1.022177	1.074021	1.065294	1.139849	1.018084	1.019210	1.026206
ψ	0.408174	0.464251	0.365334	0.430477	0.278300	0.201800	0.174759
δ_ψ	0.027668	0.020351	0.031363	0.026778	0.038266	0.046406	0.056106
δ_ν	0.009345	0.005577	0.009625	0.009152	0.008358	0.004965	0.008549
ξ	0.000010	0.000019	0.000014	0.000019	0.000016	0.000015	0.000015
Υ	-1.300000	-1.298811	-1.163236	-1.192233	-1.294551	-1.296004	-1.264257
δ_η	0.009996	0.009982	0.009908	0.009984	0.009975	0.009791	0.009678
p	0.872852	0.835976	0.954061	0.851628	1.101173	1.267972	1.466726
q	0.146307	0.172207	0.157213	0.156613	0.126482	0.132410	0.115100

Table A. 3: Tabulated Parameters for (2) 16d (0.162" diameter by 3.5" long) WPC to Lumber Connections

Parameter	Test Run				
	1	2	3	4	5
α	0.058827	0.060000	0.059953	0.052228	0.059719
β	1.599171	1.764572	1.730684	1.758026	1.574186
ω	1.199874	1.199880	1.199993	1.199916	1.199855
ζ_0	0.967446	0.968954	0.969577	0.967402	0.969367
n	1.003487	1.002244	1.006005	1.001643	1.000097
ψ	0.102910	0.102121	0.170730	0.100419	0.100023
δ_ψ	0.062869	0.057824	0.039730	0.066095	0.066754
δ_ν	0.000007	0.000003	0.000012	0.000020	0.000000
ξ	0.000010	0.000018	0.000012	0.000011	0.000013
Υ	-1.099082	-1.264214	-1.230550	-1.257034	-1.074098
δ_η	0.002571	0.002895	0.004508	0.002198	0.002044
p	0.986853	1.022988	0.832433	1.013921	0.843740
q	0.178293	0.190149	0.221987	0.198838	0.194618

Table A. 4: Tabulated Parameters for 8d (0.131" diameter by 2 .5" long) Sheet Metal to Lumber Connections

Parameter	Test Run						
	1	2	3	4	5	6	7
α	0.023560	0.020934	0.020351	0.020254	0.021916	0.020447	0.020026
β	1.711528	1.831357	1.827785	1.795242	1.787754	1.846765	1.805485
ω	1.196346	1.185740	1.197991	1.189049	1.198626	1.189564	1.196332
ζ_0	0.969250	0.959418	0.965678	0.966942	0.968659	0.968492	0.963164
n	1.021135	1.043976	1.002213	1.000000	1.026367	1.004034	1.007378
ψ	0.100302	0.166388	0.174121	0.193741	0.186232	0.196172	0.125484
δ_ψ	0.099631	0.098494	0.090440	0.081338	0.079639	0.076879	0.096686
δ_ν	0.003269	0.002714	0.006641	0.009433	0.007917	0.009198	0.009619
ξ	0.000015	0.000012	0.000014	0.000010	0.000019	0.000012	0.000013
Υ	-1.198402	-1.283105	-1.295910	-1.288645	-1.284958	-1.275240	-1.291964
δ_η	0.006664	0.008532	0.006410	0.008721	0.008558	0.008326	0.008703
p	1.518350	1.587532	1.600000	1.567537	1.534066	1.586805	1.598266
q	0.090826	0.080928	0.089997	0.076439	0.064810	0.086192	0.097688

Table A. 5: Tabulated Parameters for 8d (0.131" diameter by 2 .5" long) OSB to Lumber Sandwiching Sheet Metal Connections

Parameter	Test Run						
	1	2	3	4	5	6	7
α	0.022841	0.020225	0.020085	0.020713	0.021428	0.022120	0.022531
β	1.877573	2.086095	1.978399	2.375731	2.017914	1.989585	1.809009
ω	1.059934	1.199622	1.080479	1.173014	1.171841	1.159852	1.200000
ζ_0	0.967450	0.948018	0.962979	0.969285	0.961718	0.948387	0.963270
n	1.020037	1.036934	1.004670	1.020336	1.001642	1.088424	1.043440
ψ	0.327074	0.190203	0.267578	0.404326	0.186922	0.234675	0.137534
δ_ψ	0.052442	0.092970	0.073251	0.024341	0.080723	0.084656	0.099850
δ_ν	0.002196	0.001887	0.003564	0.003688	0.001651	0.000699	0.007959
ξ	0.000014	0.000015	0.000016	0.000011	0.000014	0.000011	0.000012
Υ	-1.247796	-1.296026	-1.257564	-1.250262	-1.260170	-1.262369	-1.298105
δ_η	0.005304	0.009059	0.005987	0.009591	0.006598	0.008599	0.003709
p	1.322585	1.566619	1.289644	1.216896	1.596237	1.497250	1.407093
q	0.095380	0.102376	0.114846	0.137877	0.110164	0.084023	0.151581

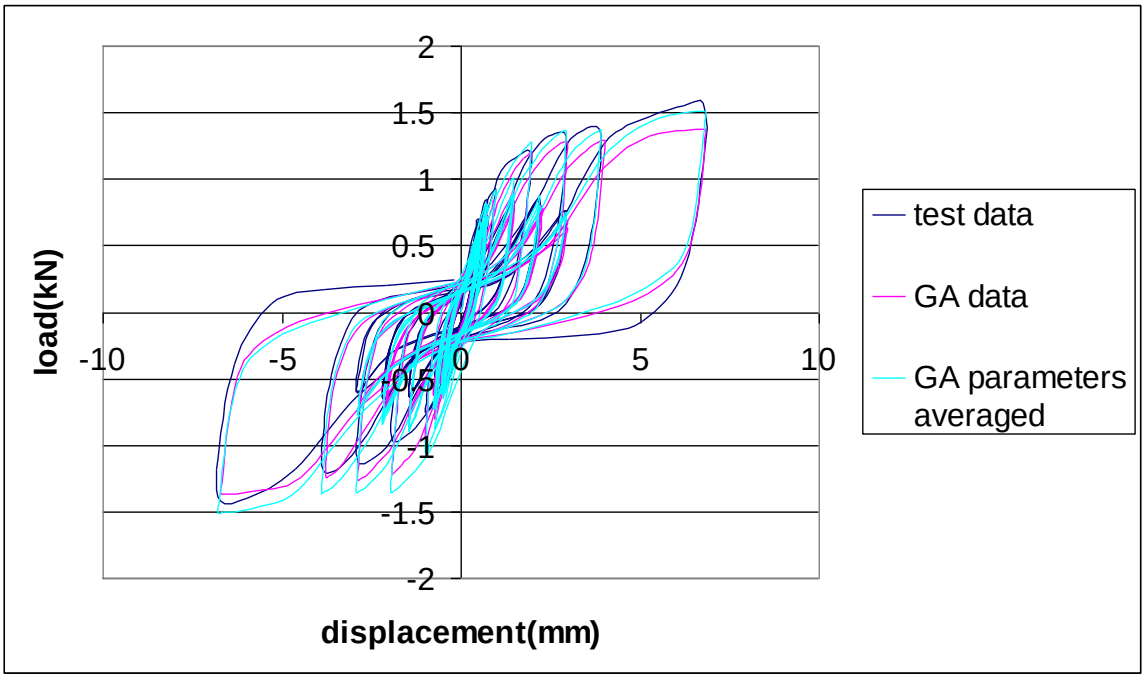

Figure A. 1: Testing Results - 8d (0.131" diameter by 2 .5" long) Nail Connecting OSB to WPC Run 1

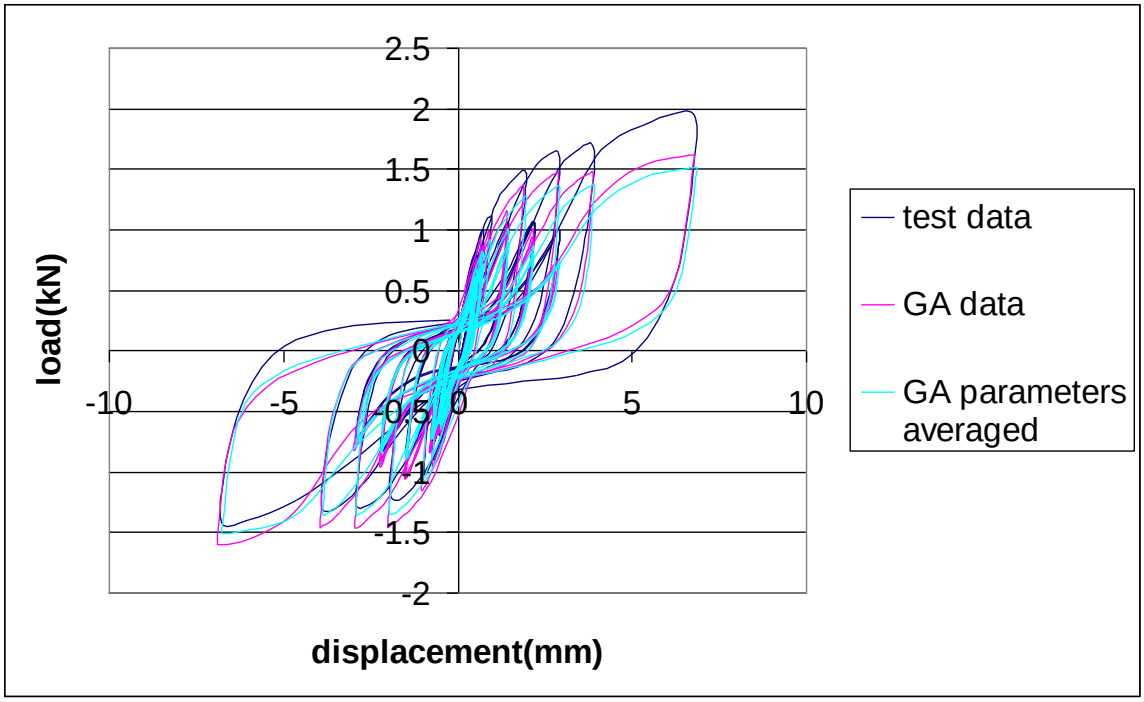

Figure A. 2: Testing Results - 8d (0.131" diameter by 2 .5" long) Nail Connecting OSB to WPC Run 2

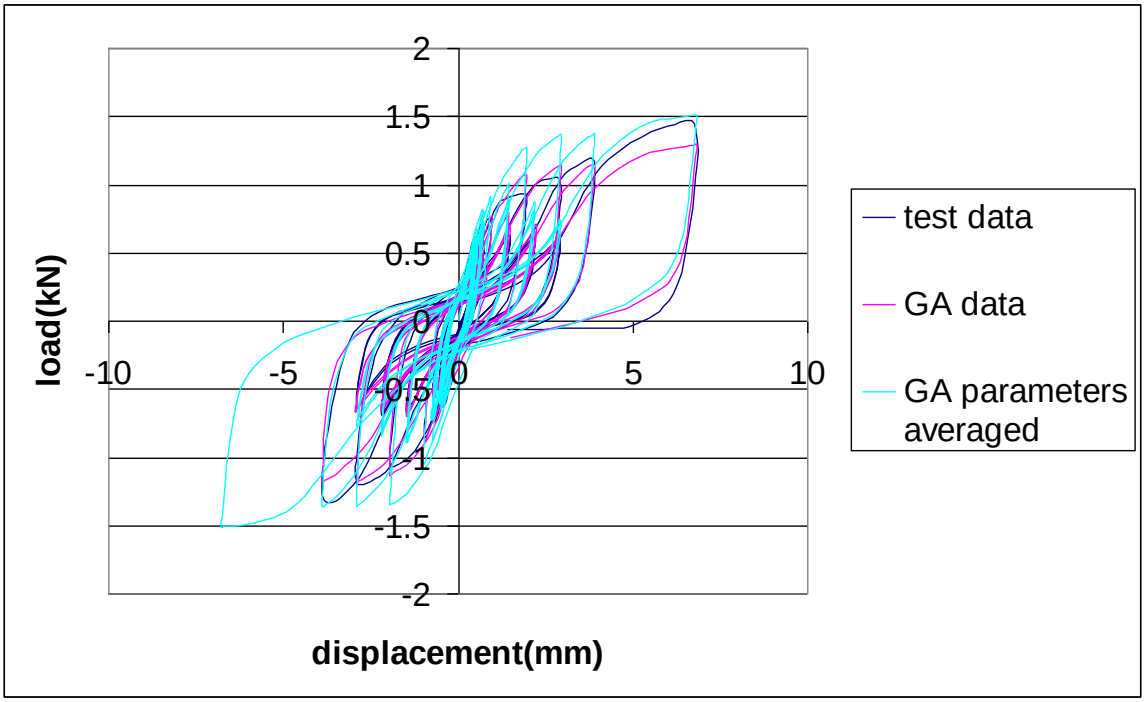

Figure A. 3: Testing Results - 8d (0.131" diameter by 2 .5" long) Nail Connecting OSB to WPC Run 3

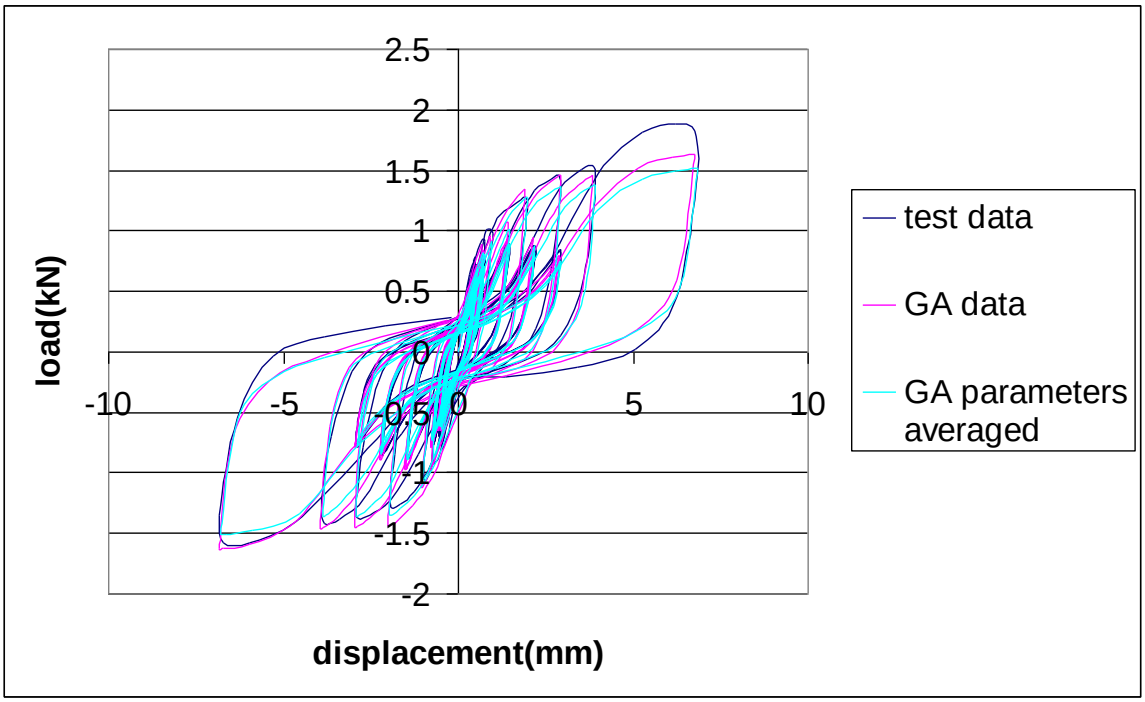

Figure A. 4: Testing Results - 8d (0.131" diameter by 2 .5" long) Nail Connecting OSB to WPC Run 4

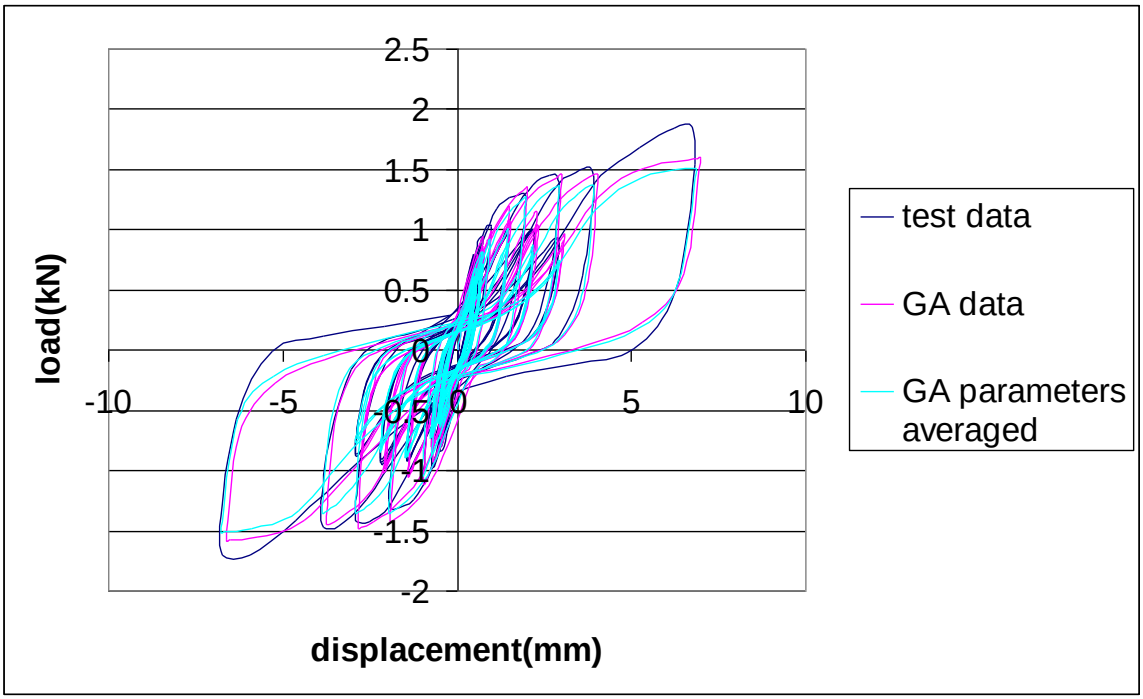

Figure A. 5: Testing Results - 8d (0.131" diameter by 2 .5" long) Nail Connecting OSB to WPC Run 5

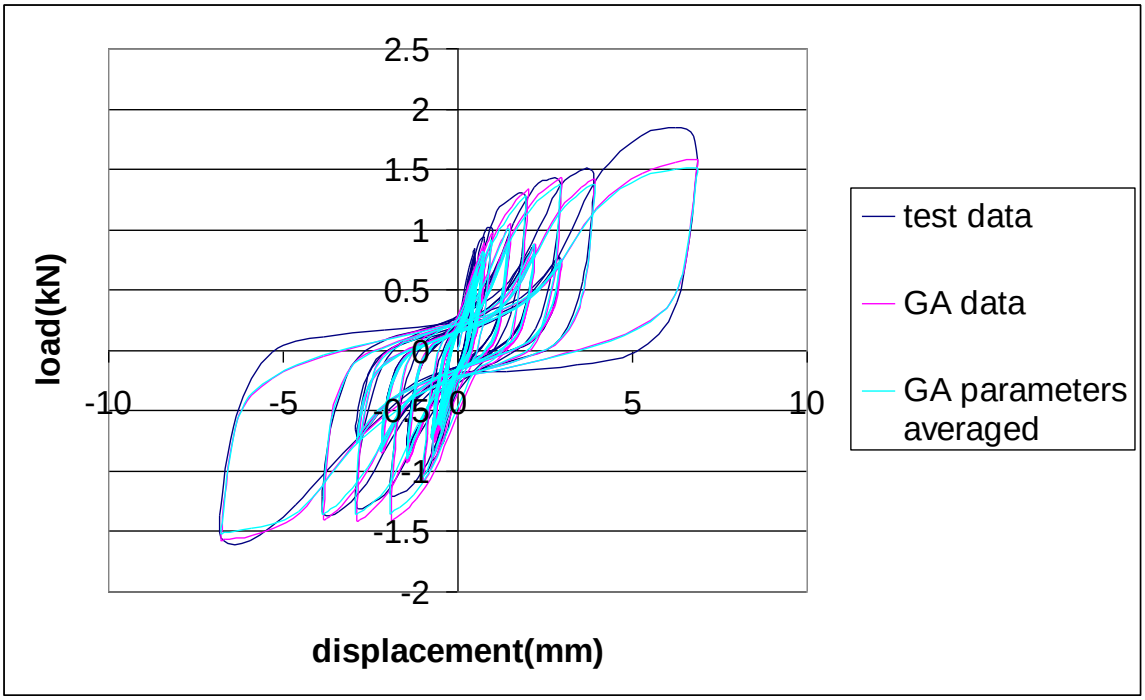

Figure A. 6: Testing Results - 8d (0.131" diameter by 2 .5" long) Nail Connecting OSB to WPC Run 6

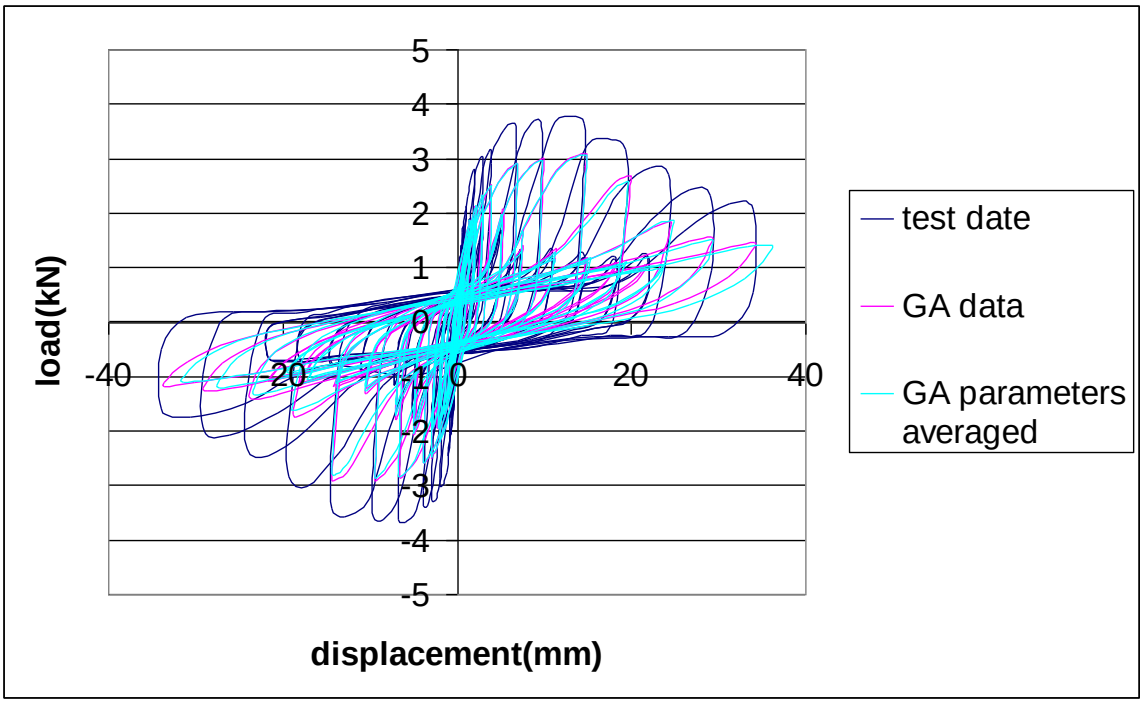

Figure A. 7: Testing Results - (2) 16d (0.162" diameter by 3.5" long) Nails Connecting WPC to Lumber Run 2

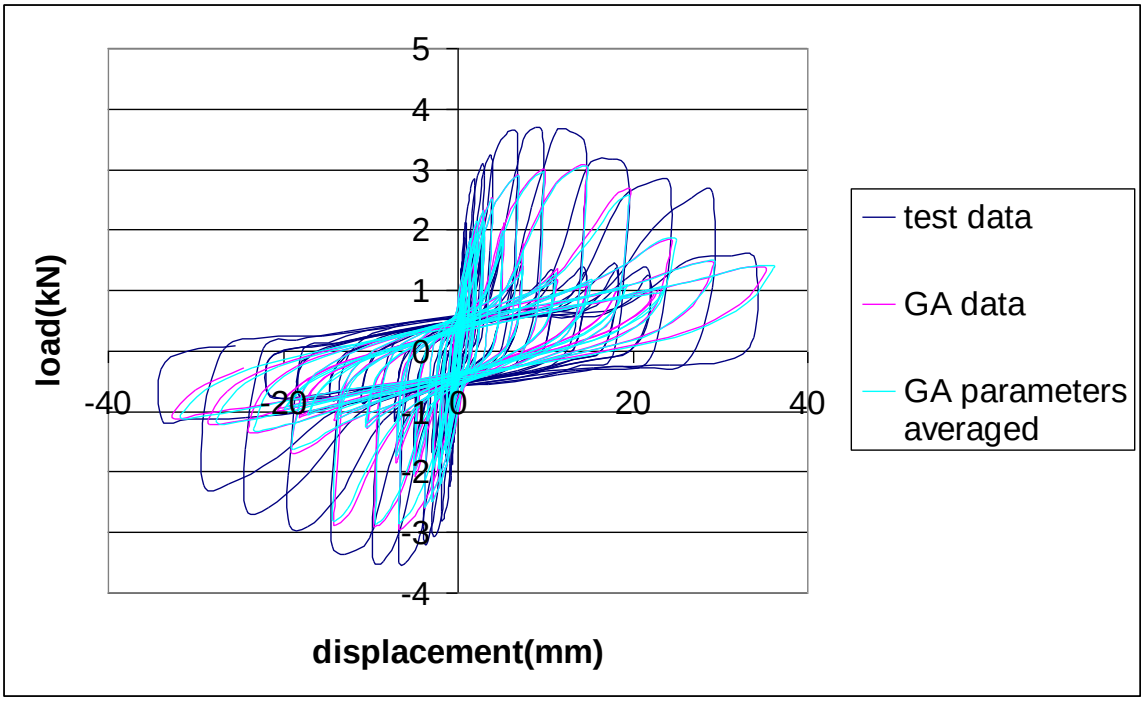

Figure A. 8: Testing Results - (2) 16d (0.162" diameter by 3.5" long) Nails Connecting WPC to Lumber Run 3

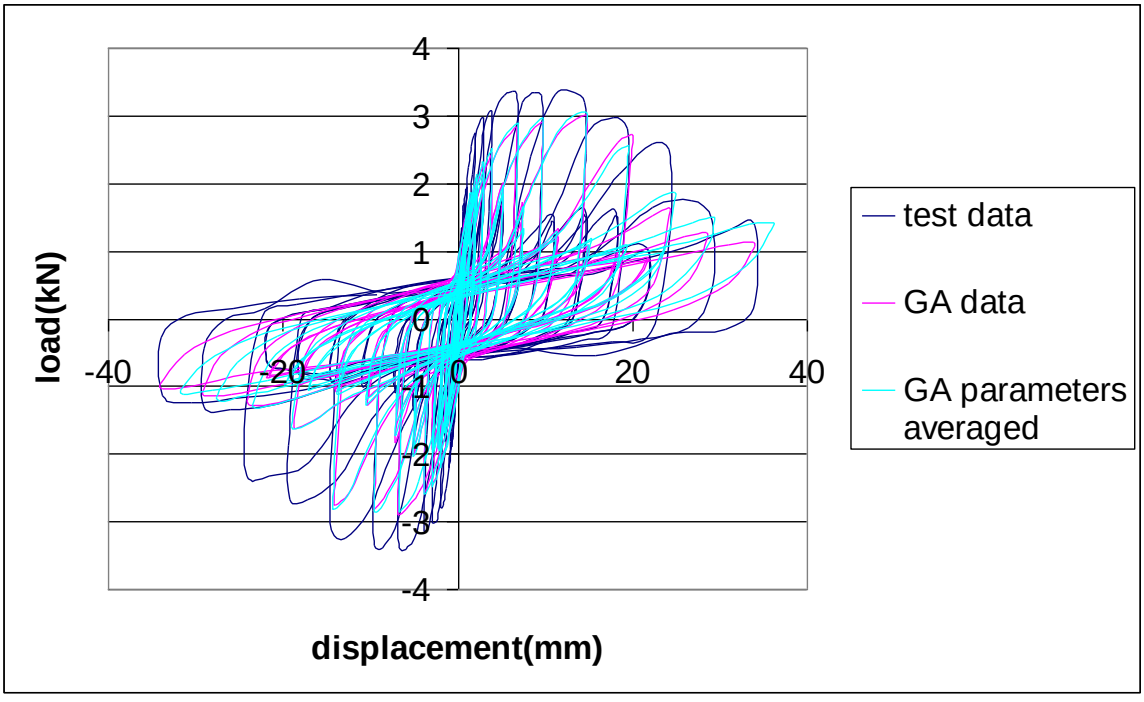

Figure A. 9: Testing Results - (2) 16d (0.162" diameter by 3.5" long) Nails Connecting WPC to Lumber Run 4

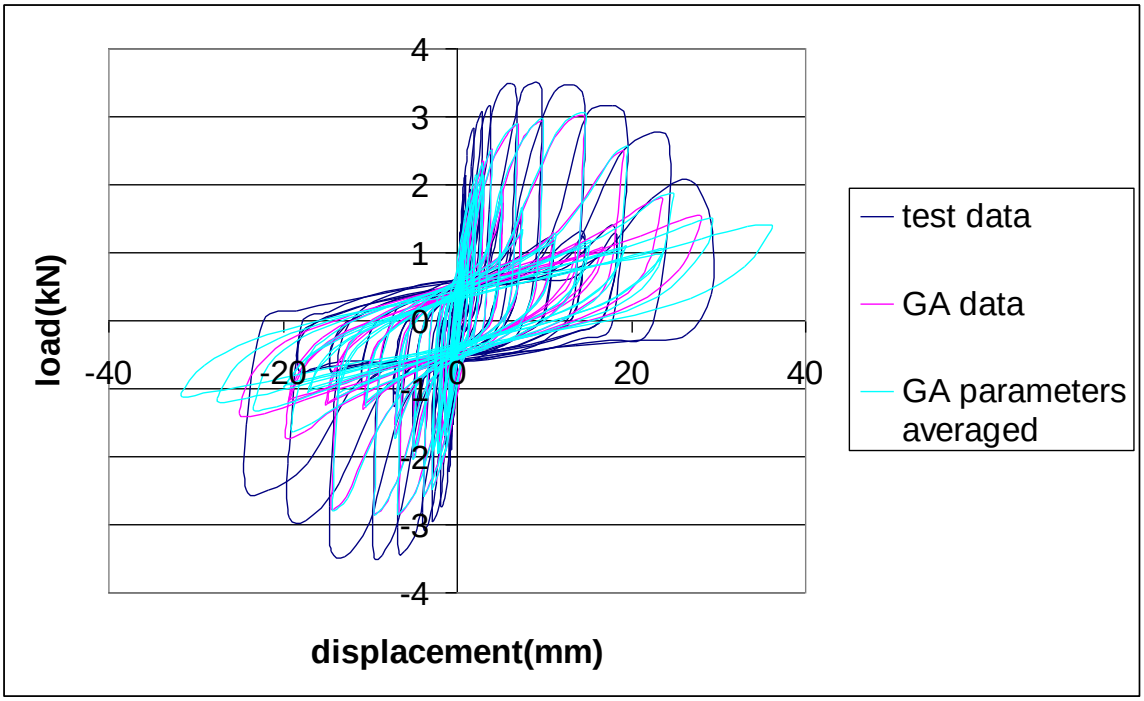

Figure A. 10: Testing Results - (2) 16d (0.162" diameter by 3.5" long) Nails Connecting WPC to Lumber Run 5

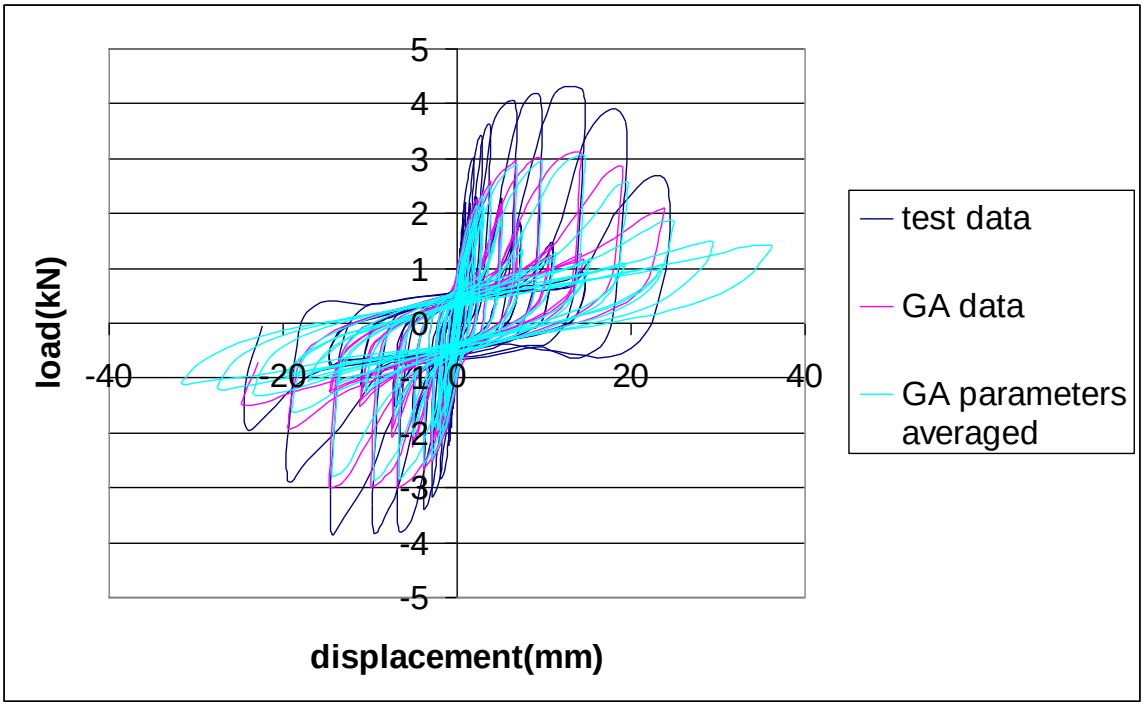

Figure A. 11: Testing Results - (2) 16d (0.162" diameter by 3.5" long) Nails Connecting WPC to Lumber Run 6

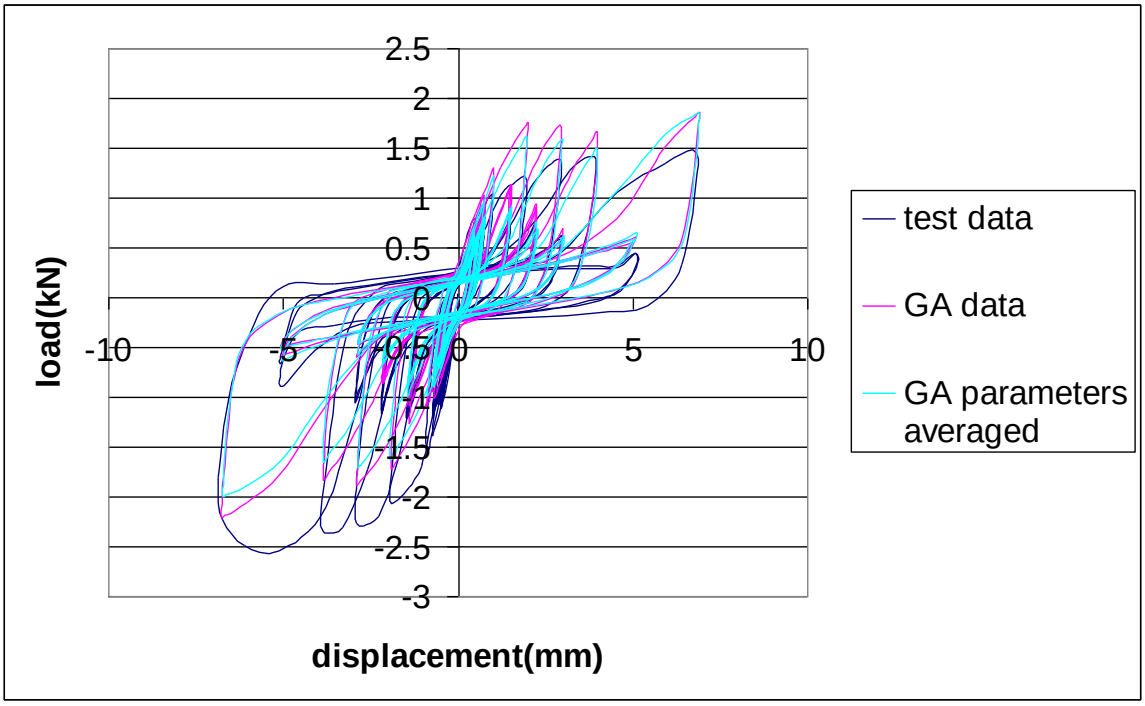

Figure A. 12: Testing Results - 8d (0.131" diameter by 2 .5" long) Nail Connecting Sheet Metal to Lumber Run 1

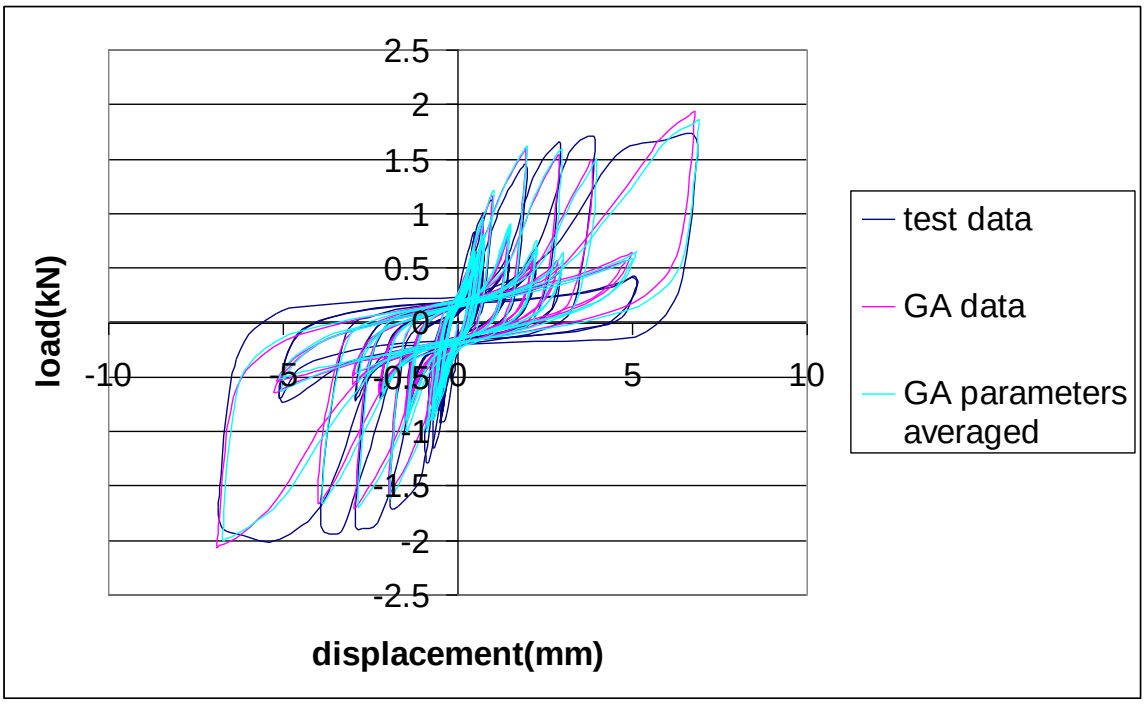

Figure A. 13: Testing Results - 8d (0.131" diameter by 2 .5" long) Nail Connecting Sheet Metal to Lumber Run 2

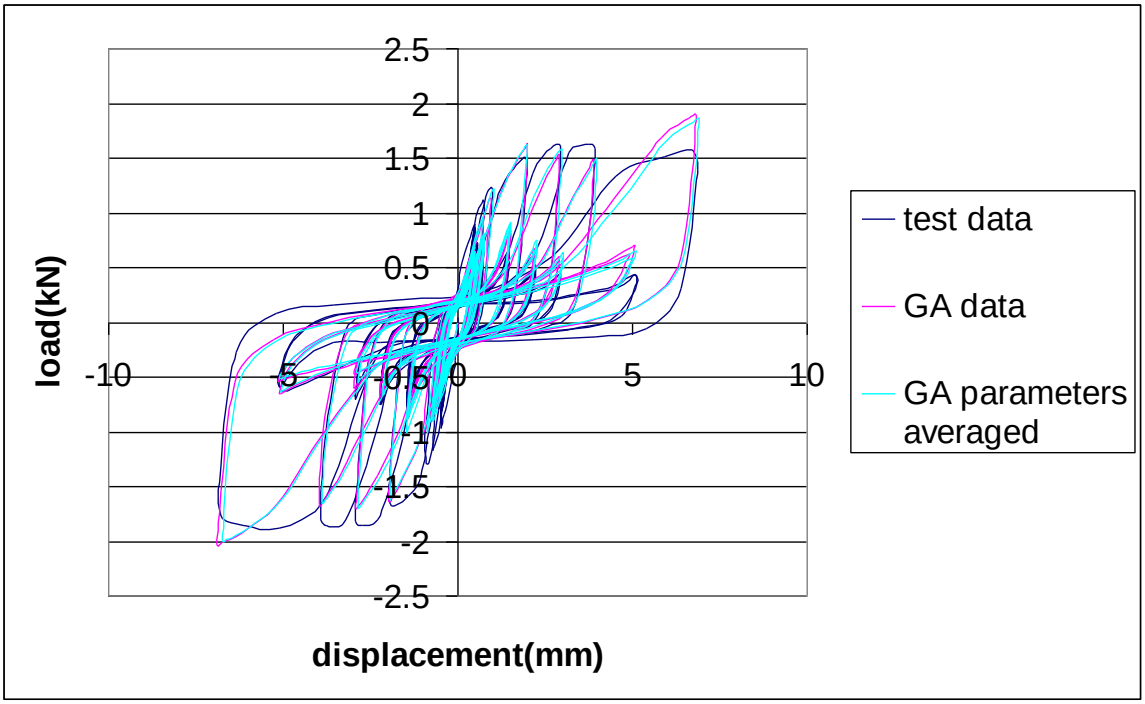

Figure A. 14: Testing Results - 8d (0.131" diameter by 2 .5" long) Nail Connecting Sheet Metal to Lumber Run 3

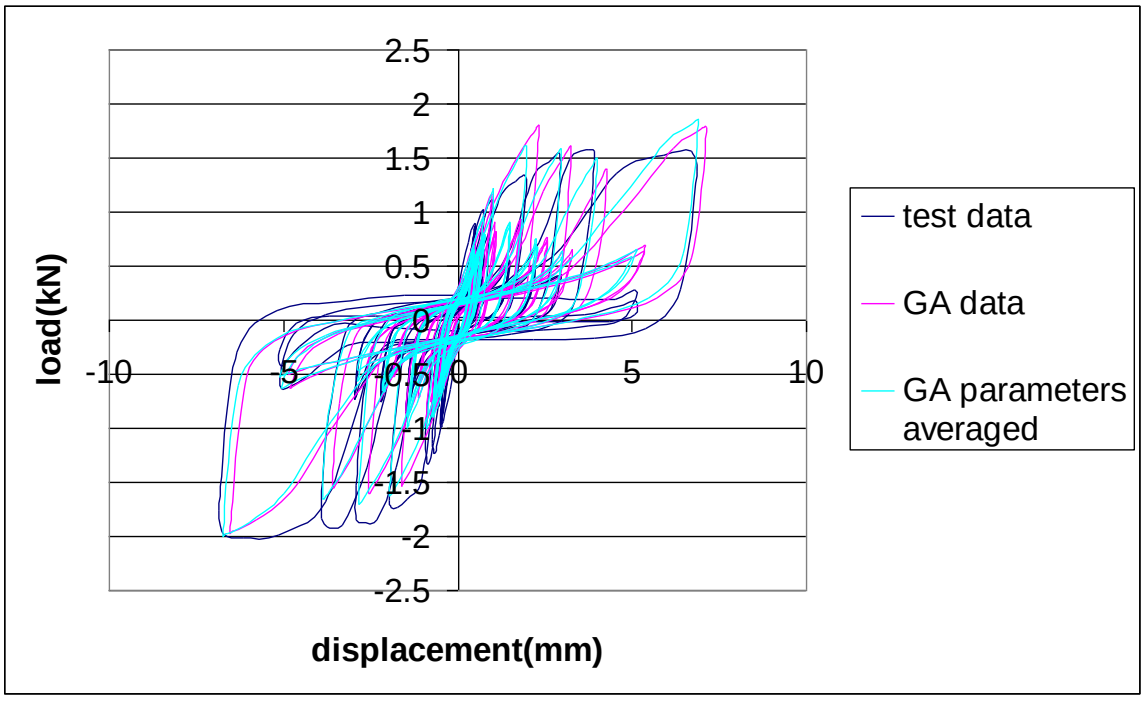

Figure A. 15: Testing Results - 8d (0.131" diameter by 2 .5" long) Nail Connecting Sheet Metal to Lumber Run 4

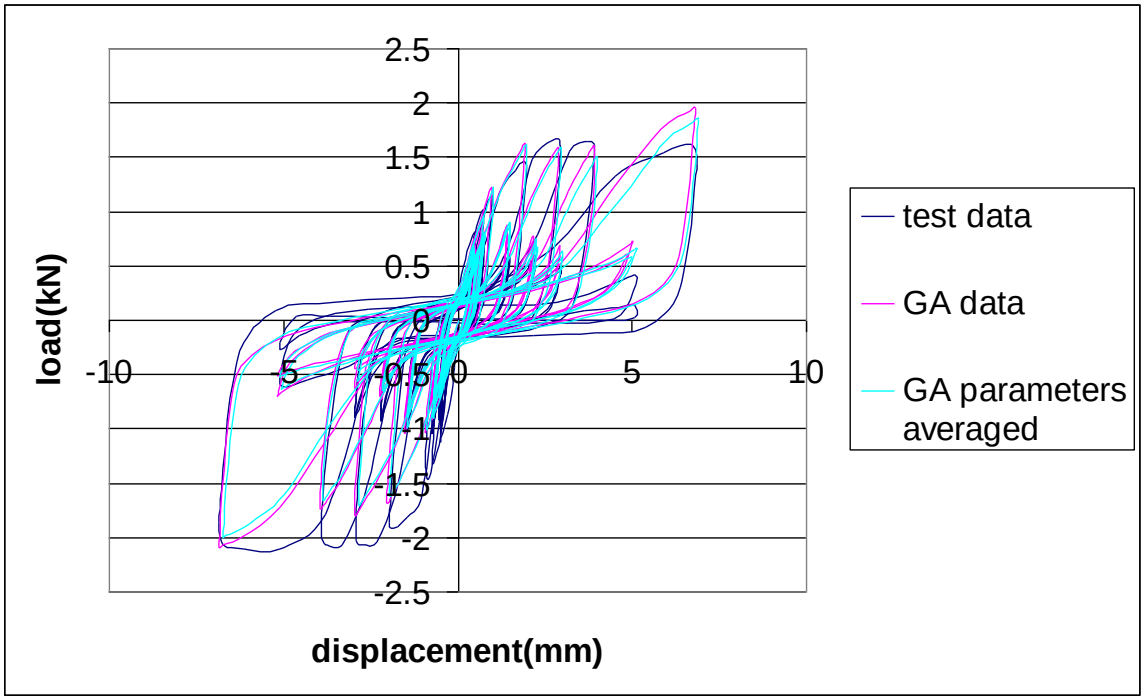

Figure A. 16: Testing Results - 8d (0.131" diameter by 2 .5" long) Nail Connecting Sheet Metal to Lumber Run 5

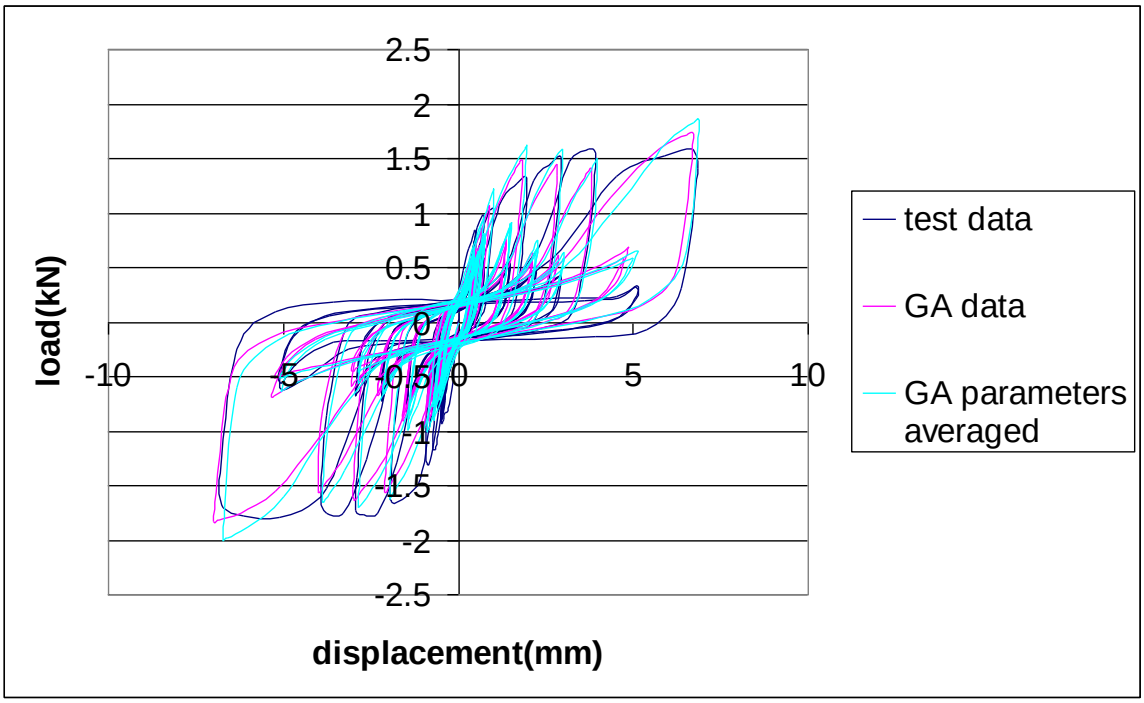

Figure A. 17: Testing Results - 8d (0.131" diameter by 2 .5" long) Nail Connecting Sheet Metal to Lumber Run 6

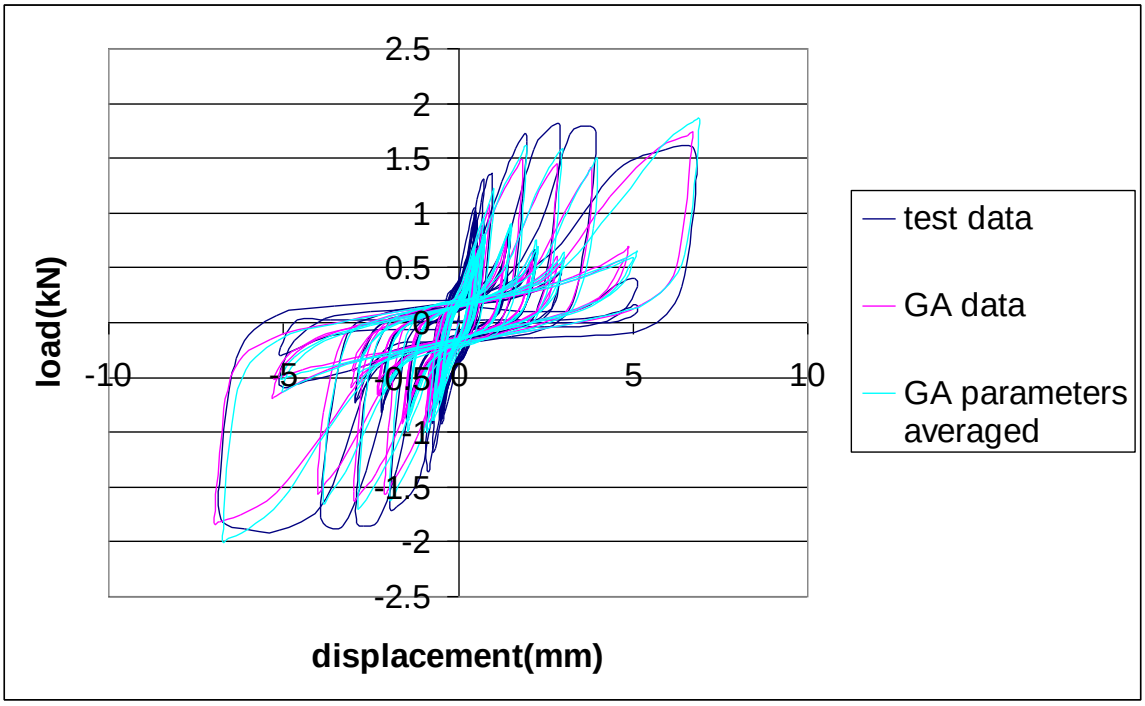

Figure A. 18: Testing Results - 8d (0.131" diameter by 2 .5" long) Nail Connecting Sheet Metal to Lumber Run 7

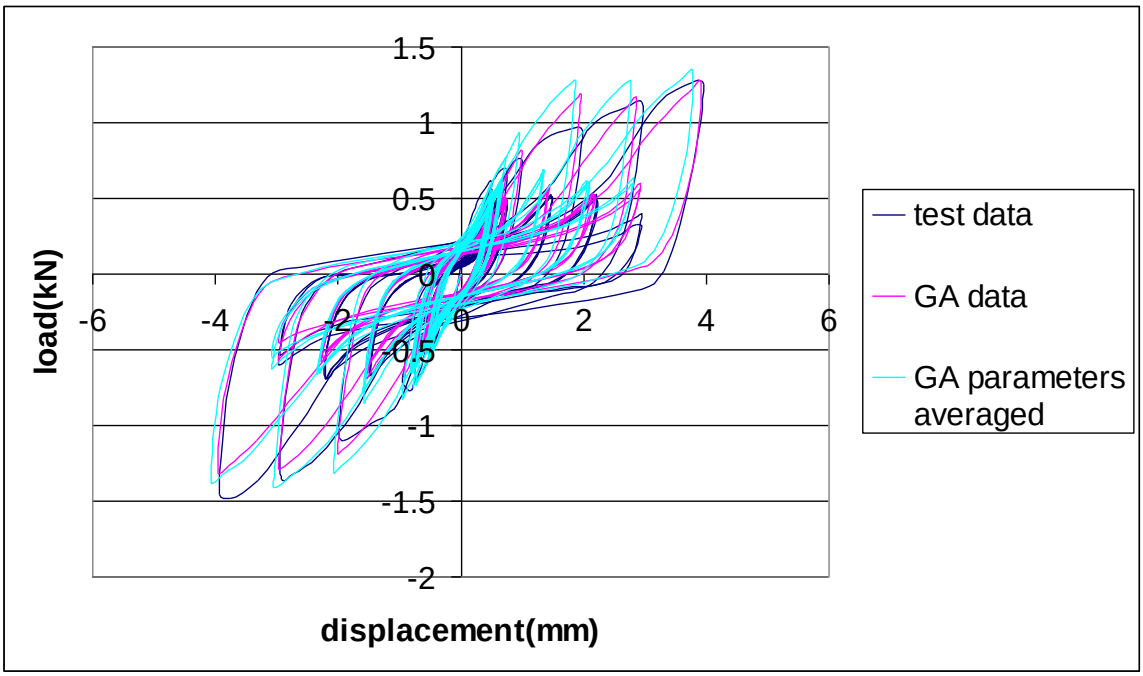

Figure A. 19: Testing Results - 8d (0.131" diameter by 2 .5" long) Nail Connecting OSB to Lumber Sandwiching Sheet Metal Run 1

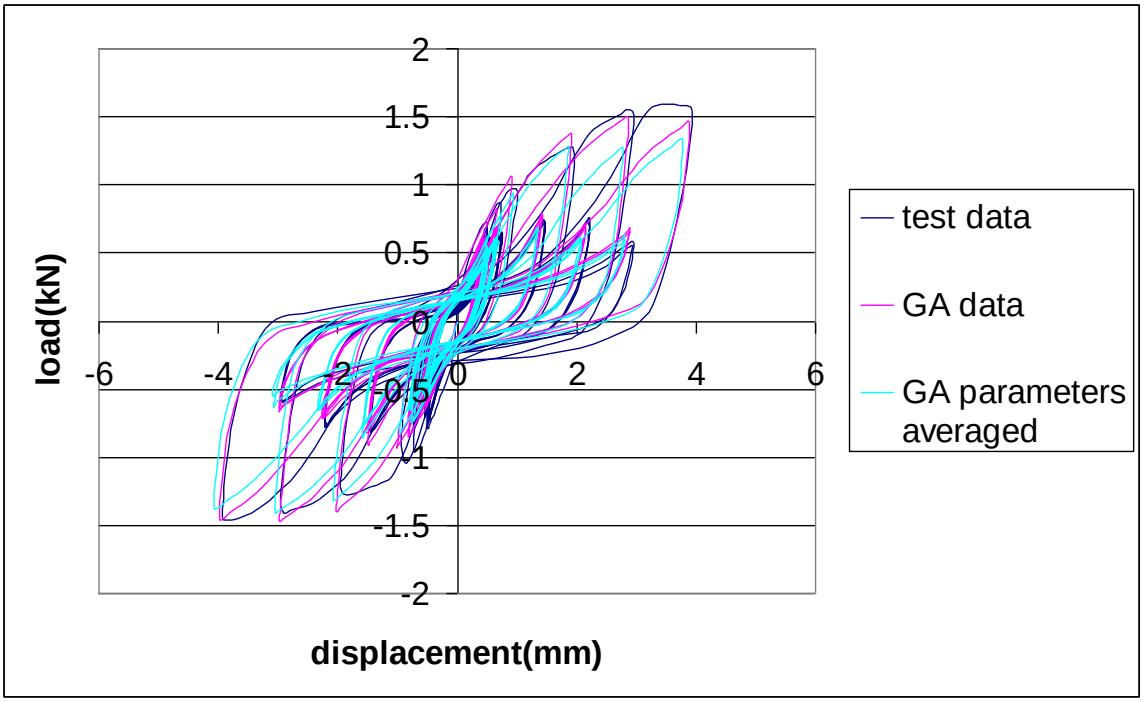

Figure A. 20: Testing Results - 8d (0.131" diameter by 2 .5" long) Nail Connecting OSB to Lumber Sandwiching Sheet Metal Run 2

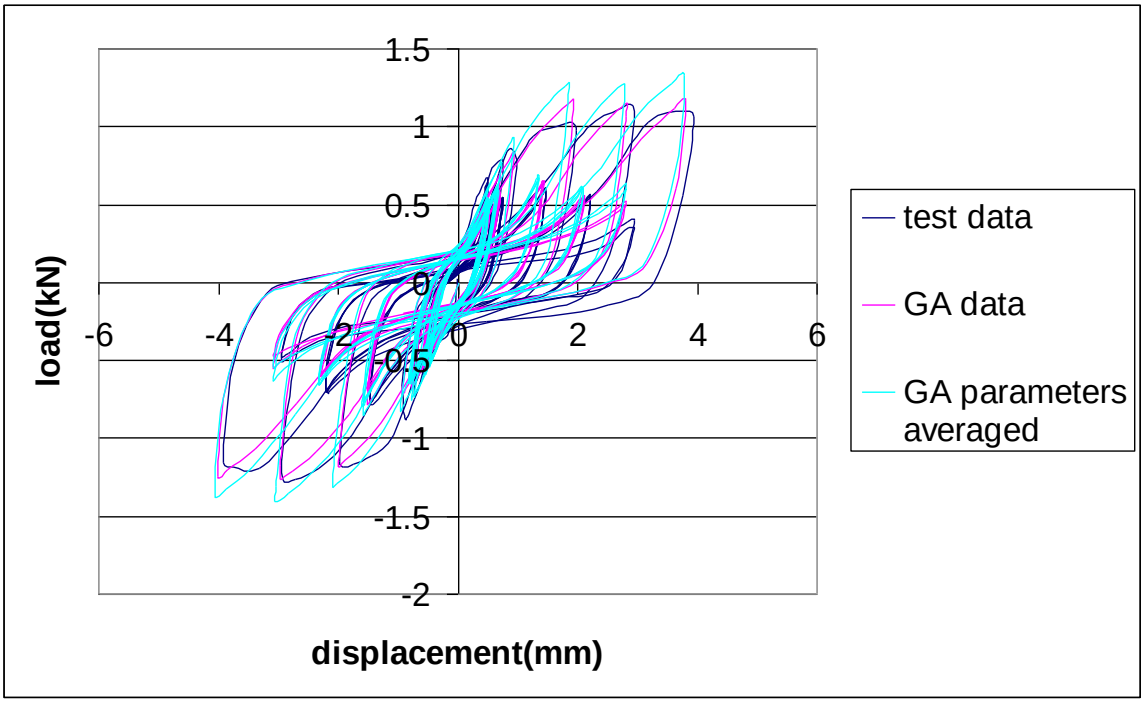

Figure A. 21: Testing Results - 8d (0.131" diameter by 2 .5" long) Nail Connecting OSB to Lumber Sandwiching Sheet Metal Run 3

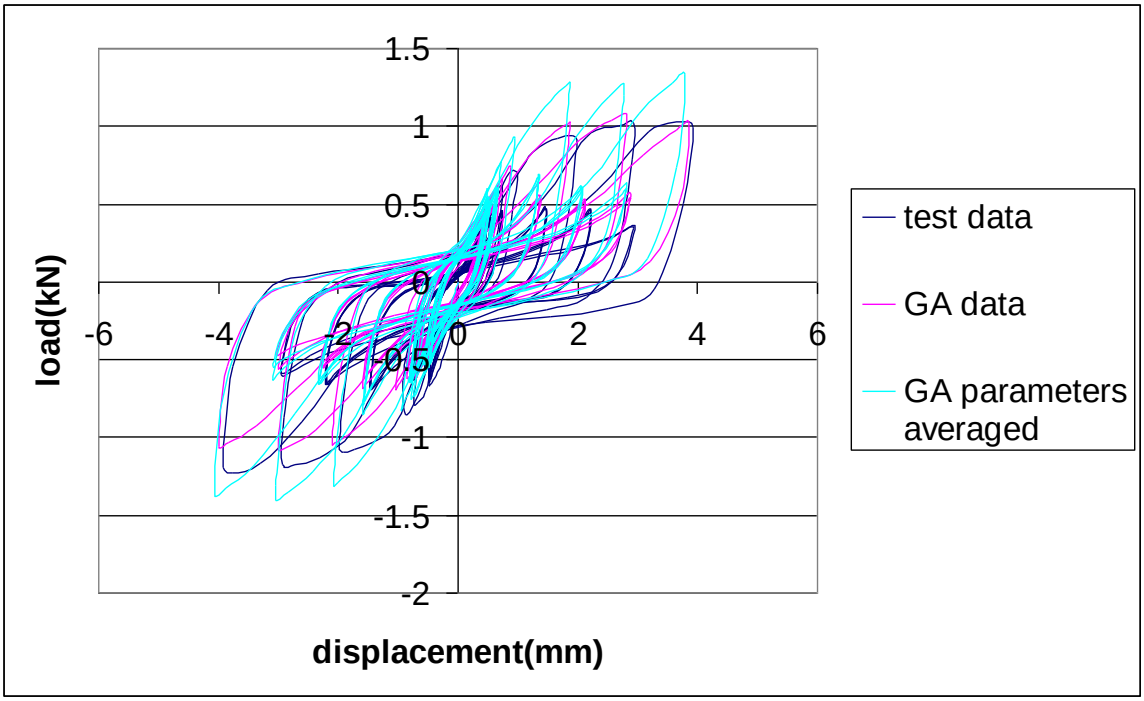

Figure A. 22: Testing Results - 8d (0.131" diameter by 2 .5" long) Nail Connecting OSB to Lumber Sandwiching Sheet Metal Run 4

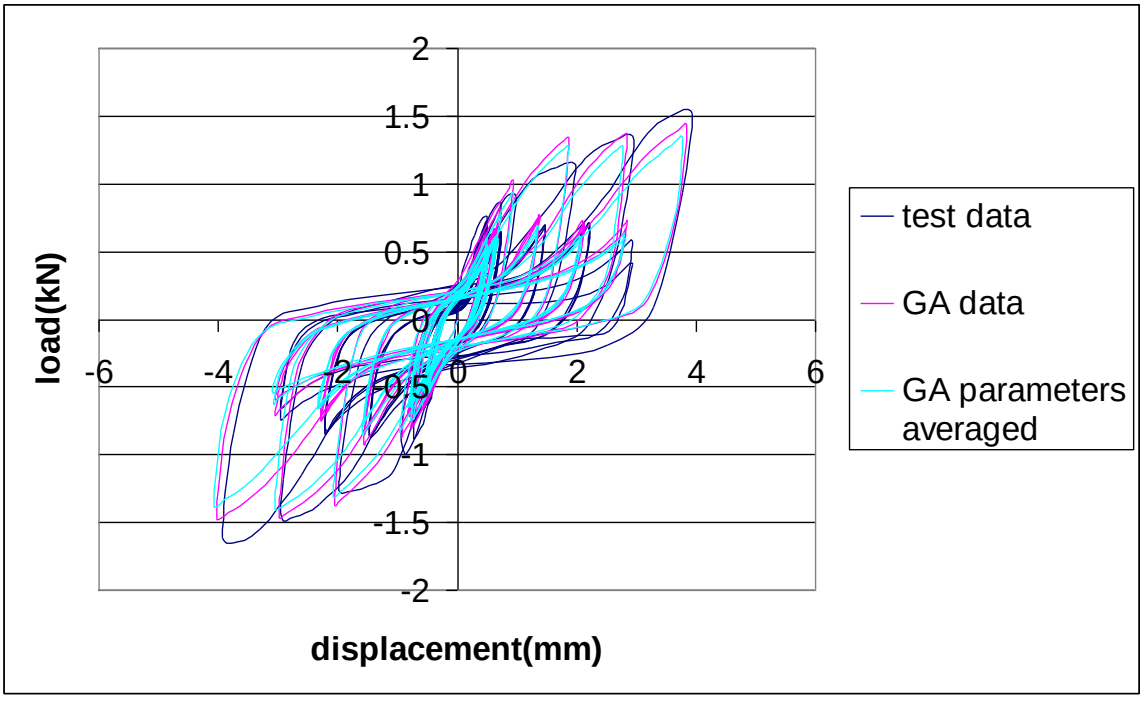

Figure A. 23: Testing Results - 8d (0.131" diameter by 2 .5" long) Nail Connecting OSB to Lumber Sandwiching Sheet Metal Run 5

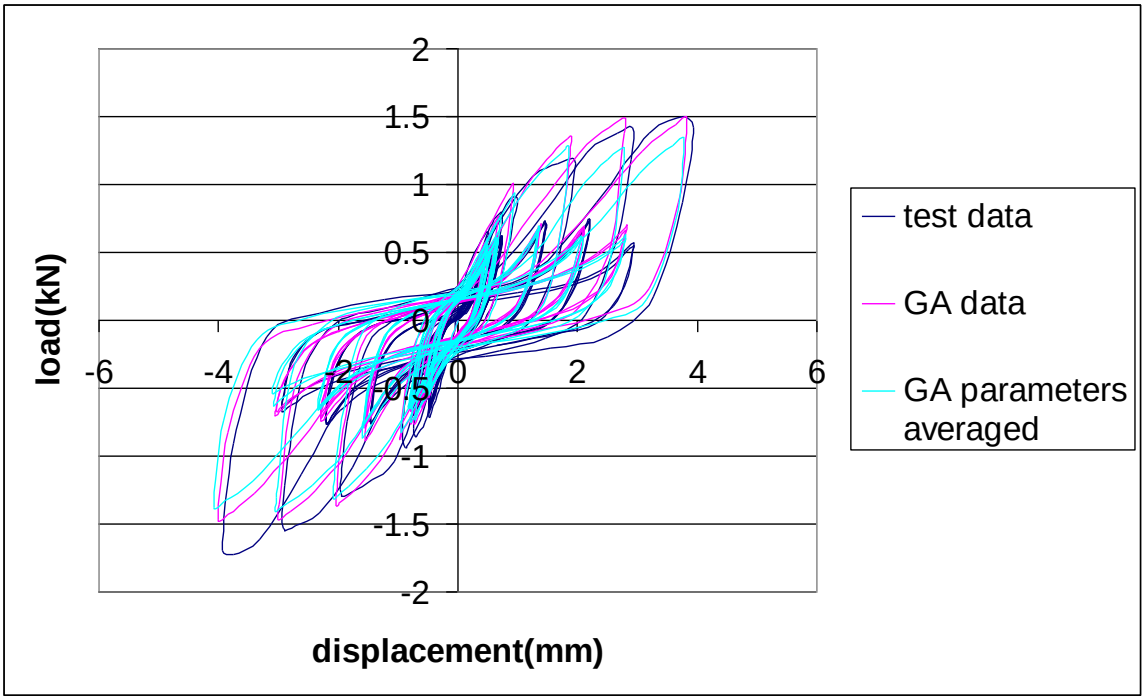

Figure A. 24: Testing Results - 8d (0.131" diameter by 2 .5" long) Nail Connecting OSB to Lumber Sandwiching Sheet Metal Run 6

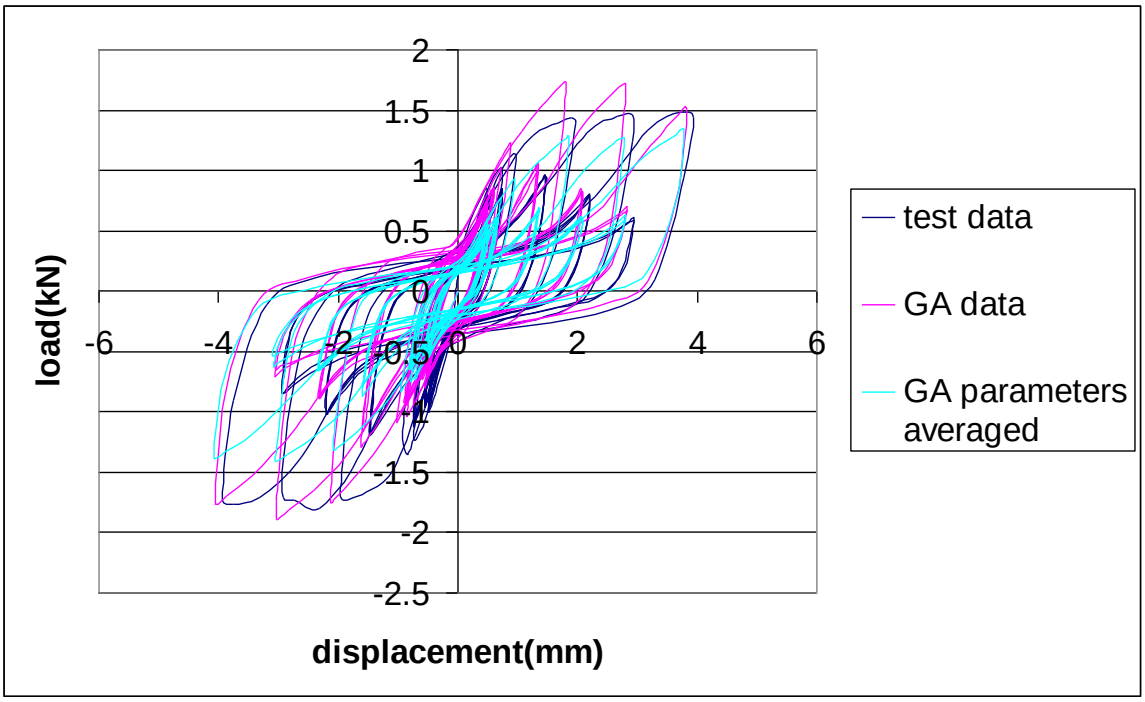

Figure A. 25: Testing Results - 8d (0.131" diameter by 2 .5" long) Nail Connecting OSB to Lumber Sandwiching Sheet Metal Run 7